

We thank both referees for their valuable comments and appreciate the associated improvements to the manuscript.

**Referee#1:**

“1. Despite continuous monitoring of N<sub>2</sub>O fluxes (Fig. 3) the authors give no values of cumulative losses per year and don't address this aspect in the discussion (see also details below). However it is quite important to interpret the impact of their findings, i.e. to which extent observed isotope fluxes are representative to agricultural ecosystems. So these numbers should be reported and discussed”

*Answer: We addressed this comment by including a corresponding paragraph in section 4.7 (see below in the response to the specific comment “Section 4.7”).*

“2. The authors use the relationship between isotope values (average d<sub>15</sub>N, d<sub>18</sub>O and SP) to estimate and discuss possible N<sub>2</sub>O reduction. While this is justified, it should be better illustrated. Instead of showing isotope maps of d<sub>18</sub>O vs d<sub>15</sub>N<sub>bulk</sub> only, they should also show SP vs d<sub>18</sub>O and also illustrate their postulated reduction events. Here I suggest to give isotope maps (SP/d<sub>18</sub>O and d<sub>15</sub>N<sub>bulk</sub>/d<sub>18</sub>O) showing the change in values during estimated reduction events. Reduction vectors could be added in these figures to show agreement or deviation of observed data from previously reported reduction dynamics. These figures might be given in the appendix.”

*Answer: We changed the manuscript accordingly and included a SP/d<sub>18</sub>O map (see below in response to the specific comment “P1590, Section 4.4”).*

P1576 L 13.14: this reasoning is not exactly correct here: independence of SP from precursors is due to the fact that N<sub>2</sub>O is the first molecule with two N atoms and thus SP is not existent in precursor compounds

*Answer: in order to be unequivocal we reworded to “..., as SP remained constant in the de novo produced N<sub>2</sub>O even though ...”*

L 26 suggest to address N<sub>2</sub>O isotopocules (or isotopologues) instead of SP since d<sub>15</sub>N<sub>bulk</sub> and not SP is used in the cited examples

*Answer: Agreed and changed to “In addition, N<sub>2</sub>O isotopocules can be used for ...”*

P1577 L 5see previous comment

*Answer: Agreed and changed to “N<sub>2</sub>O isotopomers can be ...”.*

L7 flask sampling with chambers is better in spatial resolution than atmospheric measurement (N = 1) which gives not info on spatial resolution at all

*Answer: We agree that measurements in the surface layer cannot be replicated and that for some experimental designs (e.g. different treatments on an experimental field), a chamber setup is indispensable. However, we want to raise the point that chamber measurements are representative for the usually small chamber area and are therefore limited in spatial representation. As a consequence, we changed the section to “... is limited in temporal resolution and spatial representation of a given site”.*

L 21 how about soil properties?

*Answer: In this study, measurements were made above one intensively managed grassland site for which soil properties are assumed to be constant on the timescale of this study. Therefore, an analysis with respect to variations in soil properties is not possible.*

L 22 goal (iii) can clearly not be achieved with this approach as there is no way to check the process information from isotopomers independently. Please modify accordingly or explain how you can test this with your approaches

*Answer: We agree and removed (iii) from the objectives.*

Study site: please report numbers on soil texture, Corg, C/N, pH and bulk density since these are very important to compare findings to other sites.

*Answer: We included information on bulk density, texture, pH as well as C and N content in section 2.1*

P 1579 L 16 suggest "(increase of 0.31: : : per mil.."

*Answer: Changed to "(increase by 0.31 ..... per mille ...")*

P 1583 L 21 please better explain "surface layer", lowest ten of m is quite vague, maybe add a reference here?

*Answer: The term surface layer is now explained at the beginning of section 3.2: "Air samples were taken at 2.2 m height which is in the lowest 10% of the atmospheric boundary layer (ABL) where mechanical generation of turbulence exceeds buoyant generation or consumption. This part of the ABL is called surface layer, hence corresponding air samples are referred to as surface layer air samples."*

P 1587 L 4 data are representative for this site, but not for agricultural land in general, please clarify

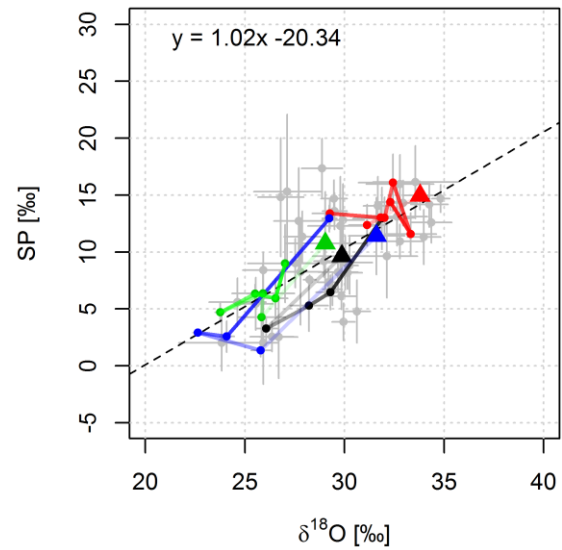
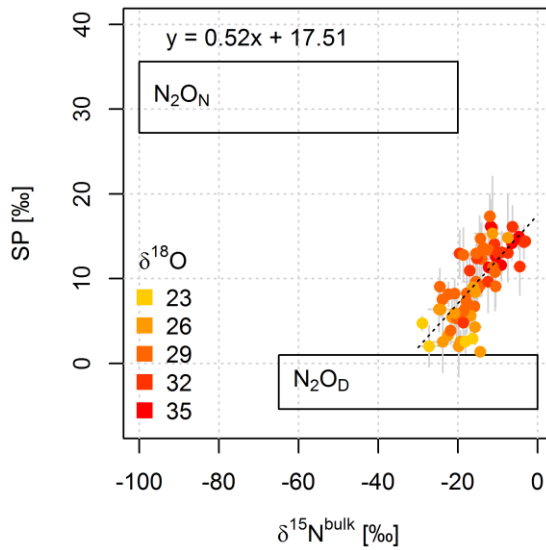
*Answer: This sentence was meant to explain that simple averages do not represent the isotopic composition of any given treatment, site or ecosystem, but we agree that our wording might be misleading. Therefore we changed to a more general term: "Representative isotopic composition of N<sub>2</sub>O emitted from a given site or treatment can be ...."*

P1590 L 8 Please add that the preferred cleavage of N-O bonds between lighter isotopes leads to increasing d18O and SP in residual N<sub>2</sub>O

*Answer: The explanation is included now: "However, in the terminal step of denitrification, namely the reduction of N<sub>2</sub>O to N<sub>2</sub>, N-O bonds between lighter isotopes are cleaved preferentially, leading to an increase in SP,  $\delta^{15}\text{N}^{\text{bulk}}$  and  $\delta^{18}\text{O}$  in the remaining N<sub>2</sub>O".*

P 1590, Section 4.4 suggest to add an SP/d18O plots (see discussion on problems of SP/d15N plots in Well et al 2012, *Geochimica et Cosmochimica Acta* 90, 265–282 Lewicka-Szczebak et al., 2014 *Geochimica et Cosmochimica Acta*, 134, 55-73, Lewicka-Szczebak et al 2015 *Rapid Comm Mass Spectrometry* 29:269-282). The extremely large range in d15N of the endmember areas make the use of d15N really difficult. Moreover, these ranges might even be larger than reported in the literature due to the unknown d15N of NO<sub>3</sub> in active microsites. Conversely, d18O of N<sub>2</sub>O produced by denitrification is mostly governed by O exchange with soil water and thus less variable.

*Answer: We agree with the referee and figure 7's right panel was substituted by a panel showing SP as a function of  $\delta^{18}\text{O}$  (see uploaded figure). We also indicated the development of isotopic composition during management events and the rewetting event as suggested by the referee in the general comments to the manuscript. The text in section 4.4 was adapted accordingly.*



L 15 to 20: please compare your endmember areas with those given and discussed in Zou et al. 2014 Soil Biology and Biochemistry, 77, 276–291.

Answer: Zou et al. give endmember areas in a SP/d15N map for the processes “Nitrification”, “Nitrifier-denitrification”, “Fungal denitrification” and “Denitrifier-denitrification”. While the SP-values representing the areas’ corner nodes are literature values, the corresponding d15N-values were calculated from the analyzed isotopic composition of N2O precursors (NO3- / NH4+) and the range of fractionation factors derived from literature for the four process groups (see table below). As our isotopocule measurements integrate over a large and (depending on wind direction) variable area, it was not possible within the scope of the presented study to sample and analyze the isotopic composition of N2O substrates. We appreciate the referee comment and the approach chosen by Zou et al., but due to the lack of knowledge on the substrate’s isotopic composition, we had to decide for a more general approach. To cover the whole range of potential d15Nbulk values, minimum and maximum values of fractionation factors reported in literature for the process groups N2O<sub>N</sub> (nitrification and fungal denitrification) and N2O<sub>D</sub> (denitrification and nitrifier denitrification) were selected and combined with the endpoints of literature values reported for the N2O precursors. Overall, as can be derived from the table below, these approaches are very much alike, but the lack of the substrate’s isotopic composition does not allow for an application of the approach chosen by Zou et al..

Study	$SP_{nit}$	$SP_{fungalDen}$	$SP_{N2ON}$	$SP_{den}$	$SP_{nit-den}$	$SP_{N2OD}$
Zou	31.4 (31.4-35.6)	37 (34.1-39.6)		-2 (-6.9-1.4)	-3.8 (-13.6-5)	
This study			$32.8 \pm 4$			$-1.6 \pm 3.8$

	$\epsilon_{nit}$	$\epsilon_{fungalDen}$	$\epsilon_{N2ON}$	$\epsilon_{den}$	$\epsilon_{NH3/NO2}, \epsilon_{NO2/N2O}$	$\epsilon_{N2OD}$
Zou	-68 to -46,9	-36.2 to -24.1		-37 to -11	-39.8 to -10.6 -39.5 to 31.4	
This study			-90 to -40			-40 to -15

L 28 here and elsewhere: BACTERIAL denitrification, since isotopologues of fungal denitrification are close to NH<sub>2</sub>OH-N<sub>2</sub>O.

*Answer: "bacterial" was added to revoke the unclear wording.*

P 1591 L 6-7 you might refer to the discussion of this aspect in Well et al 2012, *Geochimica et Cosmochimica Acta* 90, 265–282.

*Answer: Reference was added*

P1592 L10 note that N<sub>2</sub>O\_N includes Nitrification AND fungal denitrification. You can't exclude the fungi (see Sutka et al., 2008 *Rapid Commun Mass Spectrom.* 2008 3989-96,. Rohe et al., 2014 *Rapid communications in mass spectrometry*, 28, 1893-1903, please discuss).

*Answer: The section was corrected to "...due to increased contribution of nitrification or fungal denitrification, ...".*

P1593 L18 please show linearity of Keeling plots

*Answer: Keeling plots for each single day are provided as supplementary file S1, and a corresponding reference to the supplementary material was placed in the text.*

P 1994 L 6-9 not clear to me why the footprints are different, please explain

*Answer: An explanation was added in section 4.6: "Alternatively, the variation in isotope values associated with small overnight concentration increase may result from other land use or land cover. The EC fluxes are calculated from the turbulent fluctuation of concentration and vertical wind speed (i.e. the covariance of the concentration and wind speed deviations from the half-hourly mean) and therefore account for the modulation of concentration around a short term (30 min) mean caused by locally emitted N<sub>2</sub>O. Isotopic composition based on Keeling plots, however, is determined from total N<sub>2</sub>O accumulated in the nocturnal boundary layer and, thus, this approach also contains molecules that had been emitted outside the flux footprint, which almost exclusively comprised our grassland site (Zeeman et al. 2010), within the larger concentration footprint (Griffis et al., 2007)."*

Section 4.7 please discuss cumulated N<sub>2</sub>O fluxes of this site in comparison to other grassland sites in order to interpret to which extent flux weighted isotope values can be seen representative. In view of high mean fluxes it seems to me that this site is a real hot spot. (rough look at Fig 3 suggests that flux level is at least higher than 5 kg N/ha and year). This needs to be taken into account in the discussion here or at least addressed somewhere.

*Answer: We address this issue at the end of section 4.6: "Secondly, the CHA grassland can be characterized as a site with vigorous N<sub>2</sub>O emission and therefore may dominate the determined N<sub>2</sub>O isotopic composition as the influence of a source area increment scales with the source strength. The grassland was restored in 2012 which led to extraordinary high N<sub>2</sub>O-N emission of 29.1 kg ha<sup>-1</sup> year<sup>-1</sup> (Merbold et al 2014). In the following year, 2.5 kg N ha<sup>-1</sup> were released. This value is still in the range of maximum emissions reported for another intensively managed Swiss grassland, emitting 1.5-2.6 kg N ha<sup>-1</sup> year<sup>-1</sup> and at least a factor of five compared to an extensively managed grassland with less than 0.5 kg N ha<sup>-1</sup> year<sup>-1</sup> (Ammann et al 2009). With regard to distant land use and land cover, the 2.5 kg N ha<sup>-1</sup> are also more than double the median of all reported values for cultivated temperate sites and higher than the maximum value reported for forests presented in a study containing 1008 N<sub>2</sub>O emission measurements from agricultural fields (Stehfest and Bouwman, 2006)."*

P 1595 L 5 and elsewhere: add fungal nitrification since it is not distinguishable from NH<sub>2</sub>OH oxidation.

*Answer: fungal denitrification was added.*

**Referee#2:**

The manuscript reports a technical feat: the on-line isotopic characterisation of N<sub>2</sub>O emitted from an agricultural area. All descriptions, data and discussion relating to the isotopic characterisation are excellent science. A weak point is the relation of isotopic compositions to N<sub>2</sub>O flux (and soil parameters) measured on the experimental grassland plot. There are probably something like four orders of magnitude in size difference between the concentration footprint (in the order of 10 x 10 km; from which isotopic compositions were derived) and the N<sub>2</sub>O flux footprint (in the order of 0.1 x 0.1 km).

By relating changes in isotopic composition to N<sub>2</sub>O flux (and soil conditions) on the experimental grassland plot, the implicit assumption is made that N<sub>2</sub>O emitted from the grassland plot is representative, in terms of isotopic composition, for a much larger area. Looking at aerial photographs of Chamau (e.g. Google Earth), it seems there is a large proportion of arable crops and also forest within the concentration footprint (I am not familiar with this site, but think to have located it at 47 degrees 12' and 24" N and 8 degrees, 24' and 32" E). This mix of different landuse constitutes the concentration footprint and is the source of observed changes in the isotopic composition observed during nocturnal inversions. In contrast, the N<sub>2</sub>O flux measured by eddy covariance relates to the grassland site, where also the soil parameters (soil temperature and moisture, inorganic N) were measured. I would propose to drop the N<sub>2</sub>O flux part of the manuscript and relate observed changes in isotopic composition during nocturnal inversions solely to meteorological parameters ("wet phase" and "dry phase", as in section 3.5), which are much more likely to have been homogenous within the concentration footprint, than N<sub>2</sub>O flux or soil parameters (in particular NH<sub>4</sub><sup>+</sup>, NO<sub>3</sub><sup>-</sup>, DOC,) or management events.

*Answer: We agree with referee#2 that there is a remarkable difference in size between flux and concentration footprint and therefore the concentration footprint associated with our measurements of N<sub>2</sub>O isotopic composition certainly comprises adjacent areas differing in land use or land cover. In summary, however, we are confident, that the grassland represents a major contribution to the analyzed isotopic signature of the N<sub>2</sub>O accumulated above the grassland in the nocturnal boundary layer. To better illustrate our argumentation, but also to present potential limitations, we added the following changes to the manuscript:*

- 1) The manuscript title was changed from "First on-line isotopic characterization of N<sub>2</sub>O emitted from intensively managed grassland" to "First on-line isotopic characterization of N<sub>2</sub>O above intensively managed grassland".*
- 2) As given above in response to referee#1 (see comment to P 1994 L 6-9) an explanation was added why flux and concentration footprint are different and how this could influence N<sub>2</sub>O isotope analysis. In addition we added the following wording to the end of section 4.6: "However, it cannot be excluded that N<sub>2</sub>O isotopic signatures analyzed above the grassland were influenced by adjacent ecosystems". As well as section 4.7: "One has to keep in mind, however, that part of the observed variability may be attributed to the fact that the footprint area of the N<sub>2</sub>O isotopic composition includes areas with other land use or land cover".*
- 3) As detailed above in response to referee#1 (see comment to section 4.7) the weight of influence scales with source strength and distance so that areas of high source strength and low distance to the sample inlet have a higher influence on the determined isotopic composition. The grassland on which our measurements were carried out was restored in 2012 which caused extraordinary high N<sub>2</sub>O emission in 2012 (29.1 kg ha<sup>-1</sup>). Emissions during the measurement campaign were also distinctly elevated with up to 500 µg m<sup>-2</sup> h<sup>-1</sup> and the grassland site CHA can be considered as a site with vigorous N<sub>2</sub>O emission. In the study by Griffis et al. (2007) the shift of source signature was calculated for different concentration footprint sizes, assuming an increasing area of contributing C3 canopy. However, Griffis et al. postulated a constant source strength for C3 and C4 canopy, which is certainly not the case for CHA.*
- 4) In addition, the linearity of the Keeling plots, given in the supplementary file S1, indicates a constant source process. During the overnight concentration increase, which was used for the Keeling plots, wind speed and direction were not constant over the several, approx. 16 minute*

*intervals during which surface layer air was pre-concentrated. Consequently, influences from other grasslands, land use or land cover with different isotopic composition would result in Keeling plots that show a deviation from a linear relation of isotopic composition with 1/concentration. This is especially the case for  $\delta^{15}\text{N}_{\text{bulk}}$  as this value is most variable due to its dependence on precursor composition which can be expected to vary significantly in space. To highlight this, the following phrase was added to the text: "However, two facts indicate a major influence of the studied grassland on the determined  $\text{N}_2\text{O}$  isotopic composition: First, the  $\text{N}_2\text{O}$  isotopic composition is very stable for a noon-to-noon period as indicated by a linear relationship between individual measurements (supplementary file S1). This relationship persists even though wind speed and direction are changing and, therefore, individual  $\text{N}_2\text{O}$  isotope measurements integrating over 16 minutes sampling interval originate from different source areas."*

*Owing to the considerable source strength in combination with the strictly linear Keeling plots (given as supplementary material), we assume that the grassland studied has a major influence on the determined isotopic composition. Nonetheless, we clearly give credit to the possibility that adjacent regions may have influenced the determined  $\text{N}_2\text{O}$  isotopic composition.*

Page 1575, lines 13-15 state: "Hence, the development of adequate mitigation strategies is pertinent and requires a better understanding of the processes driving  $\text{N}_2\text{O}$  fluxes."

Please return in your discussion to this statement and try to show how the study has contributed to this goal (maybe as a follow-up to sections 4.4 and 4.5).

*Answer: As stated at the end of section 4.4, a better understanding of processes driving  $\text{N}_2\text{O}$  emission cannot be reached to date by determination of  $\text{N}_2\text{O}$  isotopic composition alone, but will need to be combined with other methods determining isotopic composition in the substrates and quantification of  $\text{N}_2$  emission.*

Minor:

Page 1576, line 22: insert space between "in" and "Toyoda".

*Answer: done*

Page 1579, line 18, and page 1594, line 22: maybe "comparability" instead of "compatibility"?

*Answer: The term "compatibility" is used to refer to the agreement between results from different laboratories, in accordance with the vocabulary for metrology (see GAW report No. 213, 2013).*

Page 1584, line 22: Results of DOC measurements are presented here, without the DOC measurements having been explained in the Methods section.

*Answer: Section 2.7 was supplemented by a corresponding paragraph*

1 **First on-line isotopic characterization of N<sub>2</sub>O ~~emitted from~~above intensively managed**  
2 **grassland**

3  
4 Running head: Real-time grassland N<sub>2</sub>O isotopic signature

5  
6 <sup>1,2</sup>Benjamin Wolf, <sup>3</sup>Lutz Merbold, <sup>3</sup>Charlotte Decock, <sup>1</sup>Béla Tuzson, <sup>1</sup>Eliza Harris, <sup>3</sup>Johan Six,  
7 <sup>1</sup>Lukas Emmenegger, <sup>1</sup>Joachim Mohn

8  
9 <sup>1</sup>Laboratory for Air Pollution / Environmental Technology, Empa, Überlandstrasse 129, CH-8600  
10 Dübendorf

11 <sup>2</sup>Institute for Meteorology and Climate Research (IMK-IFU), Karlsruhe Institute of Technology,  
12 Kreuzeckbahnstrasse 19, 82467 Garmisch-Partenkirchen

13 <sup>3</sup>Department of Environmental Systems Science, ETH Zurich, Universitaetsstrasse 2, CH-8092  
14 Zürich

15  
16 Corresponding author: Benjamin Wolf, benjamin.wolf@kit.edu, [+49 8821 183288](tel:+498821183288)

17 Keywords: N<sub>2</sub>O, isotopomers, QCLAS, source partitioning, grassland, nitrification,  
18 denitrification, N<sub>2</sub>O reduction

19 Paper type: primary research

20

21 **Abstract**

22 The analysis of the four main isotopic N<sub>2</sub>O species (<sup>14</sup>N<sup>14</sup>N<sup>16</sup>O, <sup>14</sup>N<sup>15</sup>N<sup>16</sup>O, <sup>15</sup>N<sup>14</sup>N<sup>16</sup>O, <sup>14</sup>N<sup>14</sup>N<sup>18</sup>O)  
23 and especially the intramolecular distribution of <sup>15</sup>N (site preference, SP) has been suggested as a  
24 tool to distinguish source processes and to help constrain the global N<sub>2</sub>O budget. However, current  
25 studies suffer from limited spatial and temporal resolution capabilities due to the combination of  
26 discrete flask sampling with subsequent laboratory-based mass spectrometric analysis. Quantum  
27 cascade laser absorption spectroscopy (QCLAS) allows selective high-precision analysis of N<sub>2</sub>O  
28 isotopic species at trace levels and is suitable for in-situ measurements.

29 Here, we present results from the first field campaign, conducted on an intensively managed  
30 grassland in central Switzerland. N<sub>2</sub>O mole fractions and isotopic composition were determined in  
31 the atmospheric surface layer (2.2 m height) at high temporal resolution with a modified state-of-  
32 the-art laser spectrometer connected to an automated N<sub>2</sub>O preconcentration unit. The analytical  
33 performance was determined from repeated measurements of a compressed air tank and resulted  
34 in measurement repeatability of 0.20, 0.12 and 0.11‰ for δ<sup>15</sup>N<sup>α</sup>, δ<sup>15</sup>N<sup>β</sup> and δ<sup>18</sup>O, respectively.  
35 Simultaneous eddy-covariance N<sub>2</sub>O flux measurements were used to determine the flux-averaged  
36 isotopic signature of soil-emitted N<sub>2</sub>O.

37 Our measurements indicate that in general, nitrifier-denitrification and denitrification were the  
38 prevalent sources of N<sub>2</sub>O during the campaign, and that variations in isotopic composition were  
39 rather due to alterations in the extent to which N<sub>2</sub>O was reduced to N<sub>2</sub>, than other pathways such  
40 as hydroxylamine oxidation. Management and rewetting events were characterized by low values  
41 of the intra-molecular <sup>15</sup>N site preference (SP), δ<sup>15</sup>N<sup>bulk</sup> and δ<sup>18</sup>O, suggesting nitrifier denitrification  
42 and incomplete heterotrophic bacterial denitrification responded most strongly to the induced  
43 disturbances. Flux-averaged isotopic composition of N<sub>2</sub>O from intensively managed grassland was



44  $6.9 \pm 4.3$ ,  $-17.4 \pm 6.2$  and  $27.4 \pm 3.6$  ‰ for SP,  $\delta^{15}\text{N}^{\text{bulk}}$  and  $\delta^{18}\text{O}$ , respectively. The approach  
45 presented here is capable of providing long-term datasets also for other  $\text{N}_2\text{O}$  emitting ecosystems,  
46 which can be used to further constrain global  $\text{N}_2\text{O}$  inventories.

47

## 48 1 Introduction

49 Atmospheric nitrous oxide (N<sub>2</sub>O) mole fraction is increasing since pre-industrial times  
50 predominately due to increased agricultural activity (Davidson, 2009; Mosier et al., 1998). Owing  
51 to the approximately 300 times higher global warming potential (GWP) compared to CO<sub>2</sub>, this  
52 greenhouse gas (GHG) currently accounts for 6% of total anthropogenic radiative forcing (Myhre  
53 et al., 2013). Recent estimates showed that N<sub>2</sub>O is in addition the single most important ozone-  
54 depleting substance (Ravishankara et al., 2009). Because at least 60% of total anthropogenic N<sub>2</sub>O  
55 emissions is attributed to food production (Syakila and Kroeze, 2011), growing human  
56 population and meat consumption per capita as well as biofuel production will accelerate the rate  
57 of increase in atmospheric N<sub>2</sub>O concentration. Hence, the development of adequate mitigation  
58 strategies is pertinent and requires a better understanding of the processes driving N<sub>2</sub>O fluxes. To  
59 date, nitrification, nitrifier denitrification and denitrification are considered to constitute the  
60 dominant N<sub>2</sub>O producing processes, especially in agricultural soils (Wrage et al., 2001). Other  
61 N<sub>2</sub>O source-processes such as abiotic N<sub>2</sub>O production, co-denitrification and heterotrophic  
62 nitrification have also been observed; a concise overview of observed processes is given  
63 elsewhere (Butterbach-Bahl et al., 2013). This complexity inherent in the N cycle and associated  
64 transformation processes is a major challenge in developing mitigation strategies, as attribution of  
65 N<sub>2</sub>O production to the respective processes is required to tailor target-oriented actions (Baggs,  
66 2008). Approaches for apportioning of N<sub>2</sub>O emissions to nitrification, denitrification, and N<sub>2</sub>O  
67 reduction to N<sub>2</sub> (source partitioning) have mostly relied on acetylene (C<sub>2</sub>H<sub>2</sub>) inhibition and  
68 isotope labeling (Groffman et al., 2006), but denitrification rates are underestimated by the C<sub>2</sub>H<sub>2</sub>  
69 method (Butterbach-Bahl et al., 2013; Groffman et al., 2006; Watts and Seitzinger, 2000). Isotope  
70 labeling approaches are vulnerable to incomplete diffusion of the tracer and to stimulation of  
71 process rates by the addition of the labeled substrates themselves (Groffman et al., 2006).

72 Changes in natural abundance of  $^{15}\text{N}$  and  $^{18}\text{O}$  in  $\text{N}_2\text{O}$  have been explored to investigate  $\text{N}_2\text{O}$   
73 production processes, but the determined  $\delta^{15}\text{N}$  and  $\delta^{18}\text{O}$  depend on both fractionation factors and  
74 isotopic composition of precursors, which in turn exhibit strong variations (Baggs, 2008; Bedard-  
75 Haughn et al., 2003; Heil et al., 2014; Toyoda et al., 2011).

76  $\text{N}_2\text{O}$  is a linear molecule and four main isotopic species can be discerned:  $^{14}\text{N}^{14}\text{N}^{16}\text{O}$ ,  $^{14}\text{N}^{15}\text{N}^{16}\text{O}$ ,  
77  $^{15}\text{N}^{14}\text{N}^{16}\text{O}$  and  $^{14}\text{N}^{14}\text{N}^{18}\text{O}$ . The isotopic species  $^{14}\text{N}^{14}\text{N}^{16}\text{O}$ ,  $^{14}\text{N}^{14}\text{N}^{18}\text{O}$  and  $^{14}\text{N}^{15}\text{N}^{16}\text{O}$  (or  
78  $^{15}\text{N}^{14}\text{N}^{16}\text{O}$ ) are isotopologues, while  $^{14}\text{N}^{15}\text{N}^{16}\text{O}$  and  $^{15}\text{N}^{14}\text{N}^{16}\text{O}$  are isotopomers and will be  
79 termed  $^{15}\text{N}^\alpha\text{-N}_2\text{O}$  and  $^{15}\text{N}^\beta\text{-N}_2\text{O}$  (Toyoda and Yoshida, 1999). The umbrella term isotopocule is  
80 used for both isotopomers and isotopologues. The intra-molecular distribution of  $^{15}\text{N}$  in  $\text{N}_2\text{O}$   
81 (‘site preference’;  $\text{SP} = \delta^{15}\text{N}^\alpha - \delta^{15}\text{N}^\beta$ ) has been reported to be independent of the substrate’s  
82 isotopic composition, as SP in the de novo produced  $\text{N}_2\text{O}$  remained constant even though  $\delta^{15}\text{N}$   
83 and  $\delta^{18}\text{O}$  values of both  $\text{N}_2\text{O}$  and substrates changed markedly during experiments with pure  
84 cultures (Heil et al., 2014; Sutka et al., 2003, 2006, 2008; Toyoda et al., 2005). Therefore, SP can  
85 be considered as a tracer conserving the source process information (Ostrom and Ostrom, 2011).  
86 The SP of different processes has been characterized in a number of pure-culture, mixed culture  
87 (Ostrom et al., 2007; Sutka et al., 2003, 2006; Toyoda et al., 2005; Wunderlin et al., 2012, 2013),  
88 and soil-incubation studies (Köster et al., 2011, 2013a; Lewicka-Szczebak et al., 2014; Well et  
89 al., 2006, 2008) with a compilation of data in Toyoda et al. (2011). A recent review on source  
90 partitioning and SP (Decock and Six, 2013b) concluded that SP is capable of distinguishing  
91 between the process groups  $\text{N}_2\text{O}_\text{N}$  ( $\text{NH}_2\text{OH}$ -oxidation, fungal denitrification and abiotic  $\text{N}_2\text{O}$   
92 production;  $\text{SP} = 32.8 \pm 4.0 \text{ ‰}$ ) and  $\text{N}_2\text{O}_\text{D}$  (nitrifier-denitrification and denitrification;  $\text{SP} = -$   
93  $1.6 \pm 3.8 \text{ ‰}$ ). In addition, the intramolecular distribution of  $^{15}\text{N}$ - $\text{N}_2\text{O}$  isotopocules can be used as  
94 an independent validation of the global, measurement-based bottom-up  $\text{N}_2\text{O}$  budget and has

95 already confirmed that the isotopically light sources such as agriculture and industry contribute to  
96 the increase in atmospheric N<sub>2</sub>O (Toyoda et al., 2013; Yoshida and Toyoda, 2000). Owing to the  
97 temporal and spatial variability of isotopomer ratios, it is indispensable to derive flux-weighted  
98 average values from different sources (such as ecosystems) for later use in budget analysis using  
99 box models (Kim and Craig, 1993; Perez et al., 2001; Yoshida and Toyoda, 2000).

100 ~~Intramolecular distribution of <sup>15</sup>N in N<sub>2</sub>O/N<sub>2</sub>O isotopomers~~ can be measured by mass  
101 spectrometry, but it requires discrete flask sampling with subsequent laboratory analysis. Hence,  
102 this approach is limited in temporal resolution and spatial ~~resolution~~representation of a given site.  
103 Additionally it is indirect, as information on the site-specific isotopic composition is derived from  
104 the analysis of the NO<sup>+</sup> fragment and N<sub>2</sub>O<sup>+</sup> molecular ion. Recently, a quantum cascade laser  
105 absorption spectrometer (QCLAS) capable of selective analysis of the three most abundant N<sub>2</sub>O  
106 isotopocules has been presented (Waechter et al., 2008) and its potential for in-situ measurements  
107 in conjunction with an automated pre-concentration unit has been shown (Mohn et al., 2010,  
108 2012). Here we present the results obtained from a, to our knowledge worldwide first, campaign  
109 in which the isotopic composition of N<sub>2</sub>O (SP, δ<sup>15</sup>N, δ<sup>18</sup>O) in the atmospheric surface layer was  
110 determined on-line by using an optimized state-of-the-art laser spectrometer. With the  
111 combination of N<sub>2</sub>O isotopic analysis by QCLAS, accompanying eddy-covariance based N<sub>2</sub>O  
112 flux measurements as well as monitoring of environmental conditions and inorganic nitrogen  
113 concentrations, our specific objectives for this study were: i) to demonstrate the capability of  
114 QCLAS systems for high precision isotopic analysis of (soil emitted) N<sub>2</sub>O in ambient air; ii) to  
115 investigate management and weather effects on isotopic composition and source processes; ~~iii) to~~  
116 ~~test the capability of the N<sub>2</sub>O isotopic composition for source partitioning; and iv and iii)~~ to

117 characterize the flux-averaged isotopic composition of N<sub>2</sub>O emitted from an intensively managed  
118 grassland.

## 119 2 Material and Methods

### 120 2.1 Study site

121 The agricultural research station Chamau (CHA) is located in Central Switzerland at an elevation  
122 of 400 m a.s.l.. The experiment was conducted on an intensively managed grassland belonging to  
123 CHA which is primarily used for fodder production and occasional winter grazing by sheep  
124 (Zeeman et al., 2010). The soil type is a cambisol with a bulk density of 0.97 g cm<sup>-3</sup>, 30.6 % sand,  
125 47.7 % silt and 21.8 % clay in the top 10 cm and pH of 5.7-6.2. Soil carbon and nitrogen content  
126 in the top 10 cm was 37.9 g kg<sup>-1</sup> and 4.1 g kg<sup>-1</sup> (Roth, 2006). Mean annual temperature and  
127 annual precipitation are 9.1°C and 1151 mm, respectively (Zeeman et al., 2010). Management  
128 practices aim at fodder production and consist of mowing followed by slurry application, with up  
129 to six mowing/slurry applications per year and occasional grazing of sheep and cattle in October  
130 and November. During the campaign in summer 2013, three management cycles were carried  
131 out. Harvest dates were June 6<sup>th</sup>, July 11<sup>th</sup> and August 21<sup>st</sup> and slurry was applied within 10 days  
132 after each mowing event. Nitrogen input was calculated from the applied amount of slurry  
133 brought to the field and the N concentration determined (Labor für Boden- und Umweltanalytik,  
134 Eric Schweizer AG, Thun, Switzerland) in a sample drawn from the supply to the trailing hose  
135 applicator. The applied N amounted to 30, 40 and 43.3 kg N ha<sup>-1</sup> for the first, second and third  
136 application, respectively. The grassland is re-established via ploughing and resowing  
137 approximately every 10 years. The last re-establishment event took place in 2012 (Merbold et al.,  
138 2014).

### 139 2.2 Instrumental setup for analysis of N<sub>2</sub>O isotopocule ratios

140 The four most abundant N<sub>2</sub>O isotopic species were quantified using a modified QCLAS  
141 (Aerodyne Research Inc., Billerica MA, USA) equipped with a continuous wave quantum  
142 cascade laser (cw-QCL) with spectral emission at 2203 cm<sup>-1</sup>, an astigmatic Herriott multi-pass

143 absorption cell (204 m path length, AMAC-200), and reference path with a short (5 cm) N<sub>2</sub>O–  
144 filled cell to lock the laser emission frequency (Tuzson et al., 2013). During the campaign, the  
145 QCLAS was operated in an air-conditioned trailer located 60 m west of the eddy-covariance (EC)  
146 tower. This trailer position contributes < 20 % to the main flux and is at the far side of prevailing  
147 wind direction (Zeeman et al., 2010). The sample air inlet was installed next to the inlet of the EC  
148 tower (2.2 m height). Sample air was drawn through a PTFE tube (4 mm ID) by a membrane  
149 pump (PM 25032-022, KNF Neuberger, Switzerland). Upstream of the pump, the sample air was  
150 pre-dried with a permeation drier (MD-050-72S-1, PermaPure Inc., USA). Following the pump,  
151 the pressure was maintained at 4 bar overpressure using a pressure relieve valve. Humidity, as  
152 well as CO<sub>2</sub>, were quantitatively removed from the gas flow by applying a chemical trap filled  
153 with Ascarite (7 g, 10 – 35 mesh, Fluka, Switzerland) bracketed by Mg(ClO<sub>4</sub>)<sub>2</sub> (2 x 1.5 g, Fluka,  
154 Switzerland). Finally, the sample gas was passed through a sintered metal filter (SS-6F-MM-2,  
155 Swagelok, USA) and directed to a preconcentration unit described in detail previously (Mohn et  
156 al., 2010, 2012). For an increase of N<sub>2</sub>O mixing ratios from ambient level to around 50 ppm N<sub>2</sub>O,  
157 approx. 8 litres of ambient air were preconcentrated. Afterwards, the preconcentrated N<sub>2</sub>O was  
158 introduced into the evacuated multi-pass cell of the QCLAS. Isotopic fractionation during  
159 preconcentration (increase by 0.31 ± 0.10, 0.34 ± 0.16 and 0.29 ± 0.07 ‰ for δ<sup>15</sup>N<sup>α</sup>, δ<sup>15</sup>N<sup>β</sup> and  
160 δ<sup>18</sup>O, respectively) was quantified by preconcentration of N<sub>2</sub>O with a known isotopic  
161 composition and subsequently corrected. Compatibility of N<sub>2</sub>O isotopomer analysis by QCLAS  
162 with isotope ratio mass spectrometry (IRMS) laboratories was recently demonstrated in an inter-  
163 laboratory comparison campaign (Mohn et al., 2014).

### 164 2.3 Measurement and calibration strategy

165 To ensure high accuracy and repeatability of the analytical system, a measurement and  
166 calibration strategy similar to the one presented by Mohn et al. (2012) was applied. It is based on

167 two standard gases differing in N<sub>2</sub>O isotopic composition, which were produced by dynamic  
168 dilution of pure medical N<sub>2</sub>O (Pangas, Switzerland) with defined amounts of isotopically pure  
169 (>98 %) <sup>14</sup>N<sup>15</sup>N<sup>16</sup>O (Cambridge Isotope Laboratories, USA) and (>99.95 %) <sup>14</sup>N<sup>14</sup>NO (ICON  
170 Services Inc., USA). Subsequent gravimetric dilution with high purity synthetic air (99.999 %,  
171 Messer Schweiz AG) resulted in pressurized gas mixtures with 90 ppm N<sub>2</sub>O (parts per million,  
172 10<sup>-6</sup> moles of trace gas per mole of dry air). Both standards were calibrated against primary  
173 standards which were previously measured by the Tokyo Institute of Technology (TIT, Toyoda  
174 and Yoshida) to anchor δ-values to the international isotopic standard scales. The first standard  
175 (S1, Table 1) was used as an anchor point to international δ-scale and used as input data for data  
176 analysis algorithms (see data processing). Therefore, the N<sub>2</sub>O isotopic composition of S1 was  
177 targeted to closely resemble background air. As the N<sub>2</sub>O isotopic composition of surface layer air  
178 is mainly a mixture of soil-derived and background composition, the second standard (S2, Table  
179 1) used for span correction was depleted in δ<sup>15</sup>N<sup>α</sup>, δ<sup>15</sup>N<sup>β</sup> and δ<sup>18</sup>O compared to background air in  
180 accordance with the expected terrestrial source signatures.

181 The measurement protocol started with the injection of S1, dynamically diluted to 50 ppm, the  
182 mole fraction of ambient N<sub>2</sub>O after preconcentration. After flushing the absorption cell with  
183 synthetic air, S2 was injected, also diluted to 50 ppm. For determination of the slight  
184 concentration dependence already reported (Mohn et al., 2012), S1 was injected again but at a  
185 higher mole fraction of 67 ppm (later referred to as S1<sub>h</sub>). This mole fraction represents the mole  
186 fraction expected after preconcentration of high concentration surface layer air. Subsequently, S1  
187 was injected again, diluted to 50 ppm, before the cell was filled with preconcentrated ambient  
188 N<sub>2</sub>O (A). This subroutine (S1+A) of injection of S1 and preconcentrated ambient N<sub>2</sub>O took 35  
189 minutes and was repeated three times. For an independent determination of repeatability, the



190 fourth sample was preconcentrated compressed air (target gas). During the campaign, two  
191 compressed air cylinders (C1 and C2, referred to as target gas) were used. Isotopic composition  
192 and N<sub>2</sub>O mixing ratio of both cylinders were determined in the laboratory prior to campaign start  
193 (Table 1). N<sub>2</sub>O mole fractions and isotopic composition analysed in the laboratory and at the field  
194 site agreed within their analytical uncertainty. Following target gas analysis, S1 and S1<sub>h</sub> were  
195 analyzed again. Another set of three subroutines S1+A completed one run. One complete cycle of  
196 6 ambient air samples and one compressed air sample took 340 minutes, leading to approx. 25  
197 ambient air samples being analysed during 24 hours. N<sub>2</sub>O mole fractions were determined  
198 according to Mohn et al. (2012).

## 199 2.4 Data processing

200 Data processing is based on individual mixing ratios of the four main N<sub>2</sub>O isotopic species and  
201 spectrometer characteristics as recorded by the instruments's software (TDLWintel, Aerodyne  
202 Research Inc., Billerica, MA, USA). In the first step, variations in the isotope ratios induced by  
203 drifts in the instrument working parameters during the field operation were corrected. A linear  
204 additive model explaining the deviation of isotope ratios R<sup>α</sup>, R<sup>β</sup> and R<sup>18O</sup> for repeated  
205 measurements of standard S1 from their mean value by absorption cell temperature (T1), laser  
206 temperature (T2), line position (LP) and pressure (p) was calibrated based on S1 injections. For  
207 isotope ratios of S1, S1<sub>h</sub>, S2, sample air and compressed air, these systematic deviations were  
208 corrected based on the respective values of T1, T2, LP and p. In a second step, concentration  
209 dependence of isotope ratios, determined using the measurements of S1 and S1<sub>h</sub>, was addressed  
210 with corrections (0.013, 0.028 and 0.004 ‰ ppb<sup>-1</sup> for δ<sup>15</sup>N<sup>α</sup>, δ<sup>15</sup>N<sup>β</sup> and δ<sup>18</sup>O) being in the same  
211 range as described earlier (Mohn et al., 2012). Subsequently, remaining drifts were corrected  
212 based on analysis of S1. Finally, isotope ratios were converted to δ-values using a 2-point  
213 calibration derived from corrected values of S1 and S2.

## 214 2.5 Determination of soil-emitted N<sub>2</sub>O isotopic composition

215 Isotopic composition of the source process “soil N<sub>2</sub>O emission” was derived using the Keeling  
216 plot approach (Keeling, 1958), where  $\delta$ -values measured (here in 2.2 m height) are plotted versus  
217 the inverse of N<sub>2</sub>O mole fractions. The intercept of the linear regression line can be interpreted as  
218 the isotopic composition of soil emitted N<sub>2</sub>O (Pataki et al., 2003). Therefore, determination of  
219 soil N<sub>2</sub>O isotopic composition requires an increase in N<sub>2</sub>O mole fraction. During the day,  
220 turbulence mixes surface layer air to the atmospheric background. At night, the surface layer  
221 becomes more stable and the N<sub>2</sub>O mole fraction increases, shifting isotopic composition towards  
222 its source composition. As a consequence, Keeling plots were based on noon-to-noon periods.  
223 This approach is discussed in section 4.6.

## 224 2.6 N<sub>2</sub>O Flux measurement

225 At CHA, greenhouse gas mole fractions, including N<sub>2</sub>O, are measured continuously since 2012  
226 by means of the eddy covariance (EC) method (Baldocchi and Meyers, 1998). The system  
227 consists of a three-dimensional sonic anemometer to measure wind speed and direction (2.41 m  
228 height, Solent R3, Gill Instruments, Lymington, UK) and a QCLAS (mini-QCLAS, Aerodyne  
229 Research Inc., Billerica, MA, USA) to determine N<sub>2</sub>O mole fractions at a temporal resolution of  
230 10 Hz. Both data streams are merged near-real time within a data acquisition system (MOXA  
231 embedded Linux computer; Moxa, Brea, CA, USA) via an RS-232 serial data link (Eugster and  
232 Plüss, 2010). The setup has been described in detail previously (Merbold et al., 2014). Post-  
233 processing of N<sub>2</sub>O fluxes included screening for obvious out-of-range values ( $\pm 100 \text{ nmol m}^{-2}\text{s}^{-1}$ ).  
234 N<sub>2</sub>O fluxes were further aggregated to noon-to-noon daily averages to smoothen the large  
235 variability in the 30 min flux averages. Daily averages were calculated for days where more than  
236 30 half-hour values were available, with this filter excluding three days from analysis.

237 2.7 Soil inorganic N, dissolved organic C and environmental conditions

238 Ammonium ( $\text{NH}_4^+$ ) and nitrate ( $\text{NO}_3^-$ ) concentrations were determined from soil (0-20 cm depth)  
239 sampled at 10 positions along a transect within the footprint of the EC measurements following  
240 the predominant wind direction. Samples were taken weekly throughout the campaign or daily  
241 during mowing and slurry application events. Per sample, ~15 g of fresh soil were added to  
242 specimen vessels containing 50 ml 1M KCl. After 1 hour on a shaker, the supernatant was  
243 filtered (Whatman no.42 ashless filter paper, 150 mm diameter) and analysed colorimetrically for  
244  $\text{NH}_4^+$  and  $\text{NO}_3^-$ . For a subset of extracts, we determined dissolved organic carbon (DOC)  
245 concentrations by combustion of KCl extracts using a total organic C analyzer (Shimadzu TOC-  
246 V, Columbia, MD, USA).

247 Soil temperatures and volumetric soil moisture contents at 10 cm depth were measured at the  
248 same 10 locations along the transect (5TM-sensors, Decagon Devices Ltd., Pullman, USA). Data  
249 were stored as 10 minute averages on a data logger (EM50, Decagon Devices Ltd., Pullman,  
250 USA). The volumetric water content was converted to water filled pore space (wfps) using a bulk  
251 density of  $1.09 \text{ g cm}^{-3}$ . Precipitation was measured with a tipping bucket rain gauge (Type 10116,  
252 Toss GmbH, Potsdam, Germany) and stored as 10 min averages on a data logger (CR10X-2M,  
253 Campbell Scientific Inc., Logan, USA).

254

255

## 256 3 Results

### 257 3.1 Long term precision for target gas analysis

258 System performance for N<sub>2</sub>O mole fractions and isotopic composition was determined based on  
259 repeated analysis of compressed air from target gas tanks (C1, C2). There was no significant drift  
260 in the  $\delta$ -values and N<sub>2</sub>O mole fractions, indicating stability of the applied measurement  
261 technique. Repeatability, calculated as the standard deviation ( $\sigma$ ) of 331 target gas measurements,  
262 amounted to 0.20, 0.12, 0.10, 0.12 and 0.22 ‰ for  $\delta^{15}\text{N}^\alpha$ ,  $\delta^{15}\text{N}^\beta$ ,  $\delta^{18}\text{O}$ ,  $\delta^{15}\text{N}^{\text{bulk}}$  and SP,  
263 respectively (Figure 1). Standard deviation for the N<sub>2</sub>O mole fraction of the target gas was  
264 0.25 ppb.

### 265 3.2 N<sub>2</sub>O mole fractions and isotopic composition at 2.2 m height

266 ~~N<sub>2</sub>O isotopic composition of the surface layer (lowest tens of meters above ground)~~ Air samples  
267 were taken at 2.2 m height which is within the lowest 10% of the atmospheric boundary layer  
268 (ABL) where mechanical generation of turbulence exceeds buoyant generation or consumption.  
269 This part of the ABL is called surface layer, hence corresponding air samples are referred to as  
270 surface layer air samples. N<sub>2</sub>O isotopic composition of the surface layer air samples (n = 2130)  
271 ranged from 2.5 to 16.1 ‰, -11.9 to -2.4 ‰, 37.6 to 44.6 ‰, -4.6 to 6.6 ‰, and 14.3 to 19.3 ‰  
272 for  $\delta^{15}\text{N}^\alpha$ ,  $\delta^{15}\text{N}^\beta$ ,  $\delta^{18}\text{O}$ ,  $\delta^{15}\text{N}^{\text{bulk}}$  and SP, respectively (Figure 2). Surface layer N<sub>2</sub>O mole fractions  
273 varied between 325 and 469 ppb and followed a diurnal cycle with highest values during the  
274 night when the boundary layer became more stable. Increasing N<sub>2</sub>O mole fractions were  
275 associated with decreasing  $\delta$ -values, indicating that soil emitted N<sub>2</sub>O that mixed into the surface  
276 layer was depleted in <sup>15</sup>N as compared to N<sub>2</sub>O in the atmospheric background.

### 277 3.3 Auxiliary measurements

278 Half hourly N<sub>2</sub>O fluxes were averaged from noon-to-noon ( $f_{N_2O}$ ), and ranged from -1 to 5 nmol  
279 m<sup>-2</sup> s<sup>-1</sup>. Maximum N<sub>2</sub>O fluxes coincided with an overnight build up in N<sub>2</sub>O mole fractions  
280 ( $\Delta N_2O$ ) as analysed by QCLAS and could not be attributed to slurry application events alone  
281 (Figure 3). Among the correlations of  $f_{N_2O}$  and auxiliary variables, only the one with nitrate  
282 concentration ( $r^2 = 0.18$ ) was significant ( $p < 0.01$ ). Soil water content (wfps) was modulated by  
283 precipitation and two clear states could be identified. During the “wet” part of the campaign  
284 lasting until July 7<sup>th</sup>, average wfps was with  $62 \pm 4$  % significantly (t-test,  $p < 0.001$ ) higher than  
285 the average of  $37 \pm 4$  % calculated for the remainder of the campaign (referred to as the “dry”  
286 part). Soil temperature did not show such a clear two-phase pattern, however temperatures during  
287 the first, “wet” part were with  $16.7 \pm 4$  °C significantly ( $p < 0.001$ ) lower than during the “dry”  
288 phase with  $21.2 \pm 2$  °C.

289 Background NH<sub>4</sub><sup>+</sup> and NO<sub>3</sub><sup>-</sup> concentrations were smaller than  $3 \mu\text{g g}_{\text{soil}}^{-1}$  and clearly responded to  
290 mowing and slurry application in the second and third management events. The NO<sub>3</sub><sup>-</sup>  
291 concentration was higher than the NH<sub>4</sub><sup>+</sup> concentration and peaked at 16 and  $50 \mu\text{g g}_{\text{soil}}^{-1}$ , while  
292 NH<sub>4</sub><sup>+</sup> concentration peaked at 9 and  $15 \mu\text{g g}_{\text{soil}}^{-1}$  for these two management events. In contrast,  
293 dissolved organic carbon concentrations (DOC) did not respond to management events, but were  
294 higher during the “dry” phase of the campaign ( $p < 0.001$ ).

### 295 3.4 Isotopic composition of soil-emitted N<sub>2</sub>O

296 The uncertainty of the determined source isotopic composition was estimated based on the  
297 standard error of the Keeling plot intercept and depends on the degree to which soil air  
298 accumulated in the surface layer ( $\Delta N_2O$ , Figure 4). For instance, the intercept (source) standard  
299 error ranged from 0.3 to 82 ‰ for SP. To apply the Keeling plot approach only to situations in

300 which soil air accumulated in the surface layer, only source isotopic compositions for overnight  
301 increases in N<sub>2</sub>O mole fractions of more than 12 ppb were considered in this study. This filter  
302 lead to a maximum and average ( $\mu$ ) standard error of 6.8 ( $\mu=2.2$ ) ‰, 4.5 ( $\mu=1.4$ ) ‰ and 2.2  
303 ( $\mu=1$ ) ‰ for SP,  $\delta^{15}\text{N}^{\text{bulk}}$  and  $\delta^{18}\text{O}$  isotopic source signatures, respectively.

304 During the field campaign, Keeling plot derived isotopic composition of soil-emitted N<sub>2</sub>O ranged  
305 from 1.4 to 17.3 ‰, -29 to -3 ‰ and 22.6 to 34.8 ‰ for SP,  $\delta^{15}\text{N}^{\text{bulk}}$  and  $\delta^{18}\text{O}$ , respectively. All  
306 explanatory variables except NH<sub>4</sub><sup>+</sup> and NO<sub>3</sub><sup>-</sup> were found to significantly correlate with SP (Table  
307 2). For  $\delta^{15}\text{N}^{\text{bulk}}$ , correlations with  $\Delta\text{N}_2\text{O}$ , wfps, soil temperature, DOC and NO<sub>3</sub><sup>-</sup> and for  $\delta^{18}\text{O}$   
308 correlations of f<sub>N<sub>2</sub>O</sub>,  $\Delta\text{N}_2\text{O}$ , precipitation, soil temperature and NO<sub>3</sub><sup>-</sup> were significant. However,  
309 the adjusted r<sup>2</sup> for all regressions was below 0.4; in addition, multiple explanatory variables such  
310 as NH<sub>4</sub><sup>+</sup> and NO<sub>3</sub><sup>-</sup> or wfps and temperature (Figure 5) did not increase the explained variance  
311 above this value.

### 312 3.5 Event-based data aggregation

313 As already described in the section “Auxiliary measurements”, there was a “wet” phase (n=27  
314 Keeling-plot derived N<sub>2</sub>O isotopic compositions) in the beginning of the campaign, which lasted  
315 about one month and a “dry” phase lasting about two months (n=38). Therefore, the dataset was  
316 split in two corresponding parts with averages of  $7.4 \pm 3.6$  ‰ versus  $11.1 \pm 4.2$  ‰ for SP, -  
317  $19 \pm 3.8$  ‰ versus  $-12.5 \pm 5.9$  ‰ for  $\delta^{15}\text{N}^{\text{bulk}}$  and  $28.7 \pm 2.2$  ‰ versus  $29.7 \pm 3.4$  ‰ for  $\delta^{18}\text{O}$  in  
318 the wet versus the dry phase, respectively. Averages of SP and  $\delta^{15}\text{N}^{\text{bulk}}$  were significantly  
319 different ( $p < 0.001$ ) but  $\delta^{18}\text{O}$  averages were not. Based on this simple classification, the dry  
320 phase contains rewetting events. A rewetting event was defined as a two day period starting at the  
321 day for which wfps increased. Exclusion of these rewetting events during the dry phase increased  
322 average  $\delta$ -values (n=30) as well as decreased standard deviations for SP,  $\delta^{15}\text{N}^{\text{bulk}}$  and  $\delta^{18}\text{O}$  to

323  $12.5 \pm 3.4$ ,  $-10.8 \pm 4.5$  and  $30.7 \pm 2.8$  ‰. Moreover the difference in  $\delta^{18}\text{O}$  was significant ( $p <$   
324  $0.001$ ).

325 In addition to the dry/wet classification, we also defined three subsets representing the  $\text{N}_2\text{O}$   
326 emission associated with management events of mowing followed by fertilization (“Mana I” –  
327 “Mana III”), one subset representing a rewetting event between Mana II and III (“Rewetting”)  
328 and one subset representing background (“BG”, all remaining measurements). There were two  
329 distinct rewetting events between management events II and III, but  $\text{N}_2\text{O}$  isotopic composition is  
330 only available for the first one (07/29/2014 - 07/31/2014). Isotopic compositions of soil-emitted  
331  $\text{N}_2\text{O}$  were assigned to subsets of management or rewetting if the associated flux or nutrient  
332 concentration was elevated. This classification scheme led to 3 to 7 measurements for  
333 management and rewetting events (Figure 3, underlaid in transparent blue) while 47 measurements  
334 were assigned to class BG. Boxplots for SP,  $\delta^{15}\text{N}^{\text{bulk}}$ ,  $\delta^{18}\text{O}$ , and wfps (Figure 6) showed  
335 characteristic  $\delta$ -values and wfps for management and rewetting, but not for subset BG.  
336 Measurements assigned to BG covered practically the whole range of values observed across all  
337 the other classes. Therefore, standard deviations for class BG were one order of magnitude larger  
338 than for the four other classes.

339 Statistical analysis is confounded by low and unequal sample size so that we compared  
340 exclusively the subsets management and rewetting using multiple non-parametric Wilcoxon tests  
341 after having checked homogeneity of variances using Bartlett test. For all investigated  $\delta$ -values,  
342 only differences between groups Mana II and Mana III were significant.

### 343 3.6 Averages of $\text{N}_2\text{O}$ isotopic signature for intensively managed grassland

344 Simple averages of daily isotopic composition of soil-emitted  $\text{N}_2\text{O}$  were  $9.6 \pm 4.4$ ,  $-15.2 \pm 6.0$   
345 and  $29.3 \pm 3$  ‰ for SP,  $\delta^{15}\text{N}^{\text{bulk}}$  and  $\delta^{18}\text{O}$ , respectively ( $n=62$ ). Representative isotopic signature

346 ~~for agricultural land~~composition of N<sub>2</sub>O emitted from a given site or treatment can be estimated  
347 based on flux-weighted averages of daily ~~signatures~~isotopic composition. For some noon-to-noon  
348 periods included in the above average, thus with an overnight increase in N<sub>2</sub>O mole fractions of  
349 at least 12 ppb, negative N<sub>2</sub>O fluxes were detected by the EC system ( $-0.17 \pm 2.1 \text{ nmol m}^{-2}\text{s}^{-1}$ ;  
350  $n=14$ ). This might be due to the uncertainty of N<sub>2</sub>O flux measurements, temporal averaging over  
351 positive and negative fluxes in a noon-to-noon period or different footprint regions for N<sub>2</sub>O flux  
352 and isotopic analysis (flux vs. concentration footprint). To avoid bias to the flux-weighted  
353 average of emitted N<sub>2</sub>O by either one of the above mentioned possible reasons, the weighted  
354 averages were calculated for positive flux events only. Flux weighted averages were  $6.9 \pm 4.3$ ,  
355  $-17.4 \pm 6.2$  and  $27.4 \pm 3.6$  ‰ for SP,  $\delta^{15}\text{N}^{\text{bulk}}$  and  $\delta^{18}\text{O}$  respectively ( $n=48$ ).

356



## 357 4 Discussion

### 358 4.1 Analytical performance

359 To our knowledge, only two pilot studies exist demonstrating the potential of QCLAS based  
360 analytical techniques for on-line and high-precision analysis of N<sub>2</sub>O mole fractions and isotopic  
361 composition in surface layer air. While Mohn et al. (2012) analyzed the three most abundant <sup>15</sup>N-  
362 isotopocules (<sup>14</sup>N<sup>14</sup>N<sup>16</sup>O, <sup>15</sup>N<sup>14</sup>N<sup>16</sup>, <sup>14</sup>N<sup>15</sup>N<sup>16</sup>O), Harris et al. (2014a) included the <sup>18</sup>O  
363 isotopologue (<sup>14</sup>N<sup>14</sup>N<sup>18</sup>O). In both studies, however, the instrument was located in the laboratory.  
364 Based on three weeks of measurements, Mohn et al. (2012) reported a precision of 0.24 and  
365 0.17 ‰ for  $\delta^{15}\text{N}^\alpha$  and  $\delta^{15}\text{N}^\beta$ , respectively and Harris et al. (2014a) reported 0.17, 0.19 and  
366 0.32 ‰ for  $\delta^{15}\text{N}^\alpha$ ,  $\delta^{15}\text{N}^\beta$  and  $\delta^{18}\text{O}$ , respectively, for a twelve days period. In both studies,  
367 analytical performance was determined, in accordance with the presented study, based on  
368 repeated analysis of compressed air samples. Thereby, the analytical precision reached in the  
369 presented study, was distinctly higher for  $\delta^{15}\text{N}^\beta$  and  $\delta^{18}\text{O}$  and similar for  $\delta^{15}\text{N}^\alpha$  compared to these  
370 two previous studies, even though the measurements were done under field-conditions and over a  
371 much longer, three months, period. This confirms the high level of precision associated with  
372 QCLAS based determination of N<sub>2</sub>O isotopic composition. Standard errors for Keeling plot  
373 intercepts (Figure 4) confirm that this precision is sufficient to resolve the variability of  
374 atmospheric N<sub>2</sub>O sampled close to the ground. As our instrument was located directly at the field  
375 site and measurements were conducted over a period of more than three months, our study  
376 indicates that this level of repeatability can be achieved both at long time scales and in the field.

### 377 4.2 N<sub>2</sub>O isotopic composition in the atmospheric surface layer (2.2 m height)

378 In our study,  $\delta$ -values of single preconcentrated air samples were between atmospheric  
379 background and 14.3 ‰ (SP) and -4.7 ‰ ( $\delta^{15}\text{N}^{\text{bulk}}$ ). Mohn et al. (2012) reported similar values  
380 between atmospheric background and 12 ‰ (SP) and -4 ‰ ( $\delta^{15}\text{N}^{\text{bulk}}$ ). Therefore the variation

381 observed in both studies is much higher compared to the measurements by Harris et al. (2014a)  
382 where the N<sub>2</sub>O isotopic composition deviated only slightly from atmospheric background. A  
383 consistent decrease in  $\delta^{15}\text{N}^{\text{bulk}}$  in parallel with increasing N<sub>2</sub>O mole fractions (accumulation of  
384 soil-derived N<sub>2</sub>O) confirms that the soil N<sub>2</sub>O source is depleted in  $^{15}\text{N}$ -N<sub>2</sub>O relative to ambient  
385 N<sub>2</sub>O (Toyoda et al., 2013). A similar pattern was found for  $\delta^{18}\text{O}$ ; an increase in N<sub>2</sub>O mole  
386 fraction was associated with a decrease in  $^{18}\text{O}$ -N<sub>2</sub>O, again indicating that soil emissions were  
387 depleted in  $^{18}\text{O}$ -N<sub>2</sub>O with respect to the atmospheric background. In contrast, Harris et al. (2014a)  
388 reported a decoupling of  $\delta^{18}\text{O}$  and  $\delta^{15}\text{N}^{\text{bulk}}$ . This may have been due to only marginal influence of  
389 soil-emitted N<sub>2</sub>O since the measurements were carried out in urban area and approx. 95 m above  
390 the ground. Studies on N<sub>2</sub>O derived from combustion processes indicate that some of these  
391 sources might be less depleted or even enriched in  $^{15}\text{N}$ -N<sub>2</sub>O compared to ambient N<sub>2</sub>O (Harris et  
392 al., 2014b; Ogawa and Yoshida, 2005).

### 393 4.3 Isotopic composition of soil-emitted N<sub>2</sub>O

394 SP of soil-emitted N<sub>2</sub>O observed in our study (1 to 17 ‰) is within the ranges expected for a  
395 mixture of the two process groups N<sub>2</sub>O<sub>N</sub> and N<sub>2</sub>O<sub>D</sub>, and does not necessarily indicate significant  
396 contribution of N<sub>2</sub>O reduction, an effect which is discussed further below. Isotopic composition  
397 of soil-emitted N<sub>2</sub>O has been predominately determined in laboratory incubation studies (Köster  
398 et al., 2013a, 2013b; Perez et al., 2006; Well and Flessa, 2009b; Well et al., 2006, 2008).

399 Additionally, results from field experiments using static chambers (Opdyke et al., 2009; Ostrom  
400 et al., 2010; Toyoda et al., 2011; Yamulki et al., 2001) and N<sub>2</sub>O accumulation below a snowpack  
401 have been published (Mohn et al., 2013). Based on pure culture studies SP values from 19.7 to  
402 40 ‰ and -8.7 to 8.5 ‰, were observed for N<sub>2</sub>O<sub>N</sub> and N<sub>2</sub>O<sub>D</sub>, respectively (Decock and Six,  
403 2013b). In field experiments SP was found to range between -1 and 32 ‰ (Opdyke et al., 2009), -  
404 3 and 18 ‰ (Yamulki et al., 2001), -14 and 90 ‰ (Toyoda et al., 2011) and 0 and 13 ‰ (Ostrom

405 et al., 2010). The very high SP values detected by Toyoda et al. (2011) may have resulted from  
406 extensive N<sub>2</sub>O reduction to N<sub>2</sub>, a process increasing SP,  $\delta^{15}\text{N}^{\text{bulk}}$  and  $\delta^{18}\text{O}$  (Ostrom et al., 2007).  
407 For  $\delta^{15}\text{N}^{\text{bulk}}$  and  $\delta^{18}\text{O}$ , a much wider variation as compared to SP is expected, because these  
408 variables depend both on fractionation factors, which vary among different microbial  
409 communities and depend on reaction conditions, as well as on the isotopic composition of the  
410 substrate (Baggs, 2008). Under field conditions,  $\delta^{15}\text{N}^{\text{bulk}}$  was reported to range between -17 and  
411 9 ‰ (Opdyke et al., 2009), -27 and 1 ‰ (Yamulki et al., 2001), -44 and 34 ‰ (Toyoda et al.,  
412 2011) and -18 and -15 ‰ (Ostrom et al., 2010), covering the range of -29 to -3 ‰ observed in  
413 this study. With respect to  $\delta^{18}\text{O}$ , the values of 22.6 to 34.8 ‰ detected for grassland in this study  
414 are at the lower end of measurements under field conditions (4-82 ‰).

#### 415 4.4 Changes in N<sub>2</sub>O source signatures induced by N<sub>2</sub>O reduction to N<sub>2</sub>

416 Quantitative source partitioning between process groups N<sub>2</sub>O<sub>N</sub> and N<sub>2</sub>O<sub>D</sub> based on SP is possible  
417 only when no other processes except those contained in the process groups have an influence on  
418 the site-specific N<sub>2</sub>O isotopic composition. However, in the terminal step of denitrification,  
419 namely the reduction of N<sub>2</sub>O to N<sub>2</sub>, ~~where N<sub>2</sub>O is the substrate, the~~N-O bonds between lighter  
420 ~~isotopic species is consumed~~isotopes are cleaved preferentially, leading to an increase in SP,  
421  $\delta^{15}\text{N}^{\text{bulk}}$  and  $\delta^{18}\text{O}$  in the remaining N<sub>2</sub>O. Consequently, part of the N<sub>2</sub>O originating from a  
422 combination of the two process groups, i.e. N<sub>2</sub>O<sub>N</sub> and N<sub>2</sub>O<sub>D</sub>, may have been consumed by N<sub>2</sub>O to  
423 N<sub>2</sub> reduction prior to emission.

424 For identification of processes determining N<sub>2</sub>O isotopic composition, isotopocule maps were  
425 suggested in which site preference is plotted versus the difference in substrate and product  
426 isotopic composition (Koba et al., 2009). Determination of isotopic composition in the substrates  
427 is time consuming and additionally confounded in our study by the large and varying footprint

428 area. Therefore, we present a modified isotope map of SP versus  $\delta^{15}\text{N}^{\text{bulk}}$  (Figure 7, left panel)  
429 instead of  $\Delta\delta^{15}\text{N}$ , the  $\delta^{15}\text{N}$  differences between substrate and product (i.e.  $\text{N}_2\text{O}$  gas). Rectangles  
430 for process groups  $\text{N}_2\text{O}_\text{N}$  and  $\text{N}_2\text{O}_\text{D}$  are defined by SP values given by Decock and Six (2013b)  
431 and by  $\delta^{15}\text{N}^{\text{bulk}}$  values calculated based on process fractionation factors and substrate isotopic  
432 composition. For nitrification and denitrification minimum and maximum fractionation factors of  
433 -90 to -40 ‰ and -40 to -15 ‰ were assumed (Baggs, 2008), for the isotopic compositions of the  
434  $\text{N}_2\text{O}$  precursors (i.e.,  $\text{NH}_4^+$  and  $\text{NO}_3^-$ ) a range of -20 to +10 ‰ and -25 to 15 ‰ were assumed.  
435 Koba et al. (2009) attributed a concurrent decrease in  $\delta^{15}\text{N}^{\text{bulk}}$  with increasing SP values as  
436 indicative for an increasing contribution of  $\text{N}_2\text{O}_\text{N}$ . In contrast, an increase in  $\delta^{15}\text{N}^{\text{bulk}}$  in parallel to  
437 increasing SP values (enrichment of  $^{15}\text{N}$  in the  $\alpha$ -position relative to the  $\beta$ -position), as observed  
438 in the present study, was allocated to a substantial increase in  $\text{N}_2\text{O}$  reduction to  $\text{N}_2$ . ~~For~~  
439  ~~$\epsilon^{15}\text{N}^{\text{bulk}}/\epsilon^{\text{SP}}$  of  $\text{N}_2\text{O}$  reduction, Koba et al. (2009) assumed a factor of 1.2 based on previous~~  
440 ~~publications. Our results (Our results (Figure 7) indicate that  $\text{N}_2\text{O}$  is predominately formed by~~  
441 ~~denitrification, and that deviations in the isotope values from denitrification may have been~~  
442 ~~caused by variations in the extent to which  $\text{N}_2\text{O}$  was reduced to  $\text{N}_2$ .; left panel) indicate that  $\text{N}_2\text{O}$~~   
443 ~~is predominately formed by bacterial denitrification, and that deviations in the isotope values~~  
444 ~~from denitrification may have been caused by variations in the extent to which  $\text{N}_2\text{O}$  was reduced~~  
445 ~~to  $\text{N}_2$ . Additionally,  $\delta^{18}\text{O}$  was found to be positively correlated with  $\delta^{15}\text{N}^{\text{bulk}}$ , which enforces the~~  
446 ~~interpretation that varying shares of  $\text{N}_2\text{O}$  reduction occurred because it acts on both N and O~~  
447 ~~isotopic composition (Koehler et al., 2012). It is noteworthy that based on such modified isotope~~  
448 maps, systematic changes in  $\delta^{15}\text{N}^{\text{bulk}}$  induced by systematic changes in N isotopic composition of  
449 one of the precursors  $\text{NH}_4^+$  or  $\text{NO}_3^-$  could be misinterpreted as reduction events: (Well et al.,  
450 2012).

451 The ratios of fractionation factors for  $\delta^{18}\text{O}$  and  $\delta^{15}\text{N}^{\text{bulk}}$  ( $r_{\text{O-N}}$ ) and SP and  $\delta^{18}\text{O}$  ( $r_{\text{SP-O}}$ ) during  $\text{N}_2\text{O}$   
452 reduction were suggested for estimation of the share of  $\text{N}_2\text{O}$  reduction to  $\text{N}_2$  since these ratios  
453 were found to be 2.5 and 0.2 to 0.5, respectively in laboratory incubation experiments. In addition  
454 to the SP/ $\delta^{15}\text{N}^{\text{bulk}}$  maps, SP/ $\delta^{18}\text{O}$  maps have been suggested to trace  $\text{N}_2\text{O}$  reduction to  $\text{N}_2$   
455 (Lewicka-Szczebak et al., 2014, 2015; Well et al., 2012). While  $\delta^{15}\text{N}^{\text{bulk}}$  depends on the isotopic  
456 composition of the precursor (e.g.  $\text{NO}_3^-$ ) and, thus, may vary considerably,  $\delta^{18}\text{O}$ - $\text{N}_2\text{O}$  is expected  
457 to be more stable as during both nitrification and denitrification, oxygen (O) later found in  $\text{N}_2\text{O}$   
458 may almost completely originate from water (Kool et al., 2009). Due to this almost complete O-  
459 exchange with water, relatively stable  $\delta^{18}\text{O}$  in soil water, and the observed constant ratio of  
460 fractionation factors for SP and  $\delta^{18}\text{O}$ - $\text{N}_2\text{O}$  ( $r_{\text{SP-O}}$ ), variation in the share of  $\text{N}_2\text{O}$  reduced to  $\text{N}_2$   
461 should be reflected by a linear relationship between SP and  $\delta^{18}\text{O}$ - $\text{N}_2\text{O}$  with a slope of 0.2-0.5  
462 (Jinuntuya-Nortman et al., 2008; Ostrom et al., 2007; Well and Flessa, 2009a). In this study, a  
463 linear relationship with a slope of 1.02 was found (Figure 7, right panel). Tracking the  
464 management events (ManaI to ManaIII) and the rewetting event in SP/ $\delta^{18}\text{O}$  space revealed that  
465 the onset of such an event is associated with a decrease of both SP and  $\delta^{18}\text{O}$ , gradually increasing  
466 back to approximately initial values, except for ManaII. During ManaII, no significant change in  
467 SP/ $\delta^{18}\text{O}$  occurred (Figure 7, right panel, red trace). The gradual increase in isotopic composition  
468 supports the conclusion from the SP/ $\delta^{15}\text{N}^{\text{bulk}}$  map that  $\text{N}_2\text{O}$  was mainly produced by bacterial  
469 denitrification and that variations in isotopic composition may have been caused predominately  
470 by  $\text{N}_2\text{O}$  reduction to  $\text{N}_2$ . This interpretation is in agreement with observations of isotopic  
471 composition of  $\text{N}_2\text{O}$ ,  $\text{NO}_3^-$  and  $\text{NH}_4^+$  during a rewetting event in an agricultural field (Decock and  
472 Six, 2013a). Additionally,  $\delta^{18}\text{O}$  was found to be positively correlated with  $\delta^{15}\text{N}^{\text{bulk}}$ , which

473 enforces the interpretation that varying shares of N<sub>2</sub>O reduction occurred because it acts on both  
474 N and O isotopic composition (Koehler et al., 2012). ~~We calculated these ratios~~  
475 ~~As introduced above, the ratios of fractionation factors for  $\delta^{18}\text{O}$  and  $\delta^{15}\text{N}^{\text{bulk}}$  ( $r_{\text{o-n}}$ ) and SP and~~  
476  ~~$\delta^{18}\text{O}$  ( $r_{\text{sp-o}}$ ) during N<sub>2</sub>O reduction were 2.5 and 0.2 to 0.5 in laboratory incubation experiments~~  
477 ~~(Jinuntuya-Nortman et al., 2008; Ostrom et al., 2007; Well and Flessa, 2009a). In our study,  $r_{\text{o-n}}$~~   
478 ~~and  $r_{\text{sp-o}}$  were 0.5 and 1, respectively for the whole dataset. We calculated these ratios also~~ for a  
479 subset of data for which all  $\delta$ -values (SP,  $\delta^{15}\text{N}^{\text{bulk}}$  and  $\delta^{18}\text{O}$ ) increased for two consecutive days,  
480 indicating that N<sub>2</sub>O reduction may have occurred. Such events were observed on 8 occasions. If  
481 source processes (N<sub>2</sub>O<sub>D</sub>, N<sub>2</sub>O<sub>N</sub>) contributed constantly over two consecutive measuring days,  
482 changes in the isotopic composition of emitted N<sub>2</sub>O were solely attributed to changes in the  
483 fraction of N<sub>2</sub>O reduction. Under such conditions one would expect that the ratio of the changes  
484 in  $\delta^{18}\text{O}$  and  $\delta^{15}\text{N}^{\text{bulk}}$  ( $r_{\text{o-n}}$ ) is around 2.5 and that the ratio of the changes in SP and  $\delta^{18}\text{O}$  ( $r_{\text{sp-o}}$ ) is  
485 between 0.2 and 0.5. The mean (median) ratios for  $r_{\text{o-n}}$  and  $r_{\text{sp-o}}$  for these selected events were  
486 0.69 (0.44) and 2.1 (1.16), respectively. While the high values of  $r_{\text{sp-o}}$  indicate that for instance  
487 changing physical conditions such as soil moisture may play a role in field measurements, the  
488 deviation of  $r_{\text{o-n}}$  from the value of 2.5 could either indicate that the fractionation factor for  $^{18}\text{O}$   
489 might be smaller than the one for  $^{15}\text{N}$  or that there is no correlation of fractionation factors in  
490 natural environments. This is in line with recent findings showing that apparent isotope effects  
491 associated with N<sub>2</sub>O reduction are sensitive to experimental conditions which influenced  
492 diffusive isotope effects (Lewicka-Szczebak et al., 2014, 2015). The same study also showed that  
493 fractionation factors during N<sub>2</sub>O reduction for  $^{15}\text{N}$  and  $^{18}\text{O}$  were variable (from -11 to +12 ‰ and  
494 from -18 to +4 ‰, respectively), and not predictable for field conditions yet. Therefore, to date,

495 the amount of N<sub>2</sub>O reduction prior to emission cannot be inferred with sufficient robustness from  
496 field measurements alone, without the knowledge of isotopic composition of the substrates.

#### 497 4.5 Controls on isotopic composition and event based data aggregation

498 The high temporal resolution of N<sub>2</sub>O isotopic and auxiliary measurements allowed us to  
499 investigate controls on N<sub>2</sub>O isotopic composition over the 3 months campaign period.

500 Correlations with isotopic composition were highest and positive for DOC and soil temperature  
501 (Table 2). The significant correlation with temperature for the whole campaign was due to a  
502 significant correlation during the “dry” part of the campaign. If the increase in SP was due to  
503 increased contribution of nitrification,  $\delta^{15}\text{N}^{\text{bulk}}$  should decrease due to the higher isotopic  
504 fractionation during this process. The simultaneous increase in SP,  $\delta^{15}\text{N}^{\text{bulk}}$  and  $\delta^{18}\text{O}$  revealed in  
505 Figure 7, however, indicates an increased share of N<sub>2</sub>O reduction to N<sub>2</sub> which might have been  
506 triggered by increased substrate availability (DOC) for heterotrophic denitrification. The reported  
507 effect of temperature on the N<sub>2</sub>O:N<sub>2</sub> ratio is not without any doubt, but a decrease has been  
508 observed with increasing temperature, supporting the hypothesis that N<sub>2</sub>O reduction increased as  
509 temperature rose throughout the measurement period (Saggar et al., 2013).

510 Though substrate availability has been identified as a major control on N<sub>2</sub>O source processes (see  
511 references in Saggar et al., 2013), correlations between N<sub>2</sub>O isotopic composition and NO<sub>3</sub><sup>-</sup> and  
512 NH<sub>4</sub><sup>+</sup> concentrations were low, except for the correlation with  $\delta^{15}\text{N}^{\text{bulk}}$ . The reason might be both  
513 the number of measurement points for substrate concentrations being lower compared to other  
514 explanatory variables and substrate concentrations not necessarily reflecting process or turnover  
515 rates (Wu et al., 2012).

516 The low explanatory power of all linear regressions underlines that drivers for N<sub>2</sub>O emissions are  
517 highly variable and may even change from event to event. In absence of management or

518 rewetting events (group BG), isotopic composition covered the whole range of measured values,  
519 while management or rewetting events were characterized by lower variability in isotopic  
520 composition. Values for SP,  $\delta^{15}\text{N}^{\text{bulk}}$  and  $\delta^{18}\text{O}$  were low for Mana I, rewetting and Mana III,  
521 whereas event Mana II showed increased SP,  $\delta^{15}\text{N}^{\text{bulk}}$  and  $\delta^{18}\text{O}$ . This indicates that processes  
522 must have been different for Mana II, although management was almost identical.

#### 523 4.6 Short term variation of isotopic composition

524 The Keeling plot approach is based on conservation of mass and assumes that the atmospheric  
525 concentration of a gas in the surface layer is a mixture of background atmospheric concentration  
526 and a variable amount of gas added by a source, raising the atmospheric concentration above  
527 background. The source's isotope value can be determined given that its isotope value remains  
528 constant during the observation period. In this study, we used noon-to-noon data in the Keeling  
529 plots to determine isotope values of soil-derived  $\text{N}_2\text{O}$  for the respective noon-to-noon period.  
530 Hence, the source processes underlying these  $\text{N}_2\text{O}$  emissions have to be constant on this time  
531 scale. Currently, little is known about the rate of change of  $\text{N}_2\text{O}$  source processes over time-steps  
532 of minutes to hours. However, changing relative contributions of source processes, which change  
533 the isotopic composition in soil-emitted  $\text{N}_2\text{O}$ , would be reflected by deviations from a linear  
534 relation between inverse concentration and isotopic composition. ~~As the Keeling plots showed no  
535 obvious deviations from a linear relation within our measurement precision, we conclude (1) that  
536 the use of the Keeling plot approach was valid in our study, and (2) that changes in  $\text{N}_2\text{O}$  source  
537 processes in our study site occurred at a time step of one day or more. While our data suggests  
538 that there are little or no changes in source processes underlying  $\text{N}_2\text{O}$  emissions within a noon-to-  
539 noon period, clear and distinct day to day variation in isotope values of soil derived  $\text{N}_2\text{O}$ ,  
540 especially in SP, were observed. Such changes were often strong and abrupt following  
541 management events (Mana I & III, Rewetting), indicating a significant response of microbial~~



542 ~~processes to the imposed disturbance. Larger than expected variability in isotope values was~~  
543 ~~observed in-between management events (class BG), when no obvious variation in environmental~~  
544 ~~drivers occurred. Since noon-to-noon concentration increases were very small during these~~  
545 ~~periods, part of this variability may be attributed to increased uncertainty around the intercept of~~  
546 ~~the Keeling plot. This is also reflected in the relatively large error bars around isotope values on~~  
547 ~~days when N<sub>2</sub>O fluxes were low (Figure 3). Alternatively some of the variation in isotope values~~  
548 ~~associated with these small fluxes may result from air masses not representative of the grassland~~  
549 ~~site as the concentration footprint influencing the N<sub>2</sub>O source signature is larger than the flux~~  
550 ~~footprint (Griffis et al., 2007). As the Keeling plots showed no obvious deviations from a linear~~  
551 ~~relation within our measurement precision (See supplementary file S1), we conclude (1) that the~~  
552 ~~use of the Keeling plot approach was valid in our study, and (2) that changes in N<sub>2</sub>O source~~  
553 ~~processes in our study site occurred at a time step of one day or more. While our data suggests~~  
554 ~~that there are little or no changes in source processes underlying N<sub>2</sub>O emissions within a noon-to-~~  
555 ~~noon period, clear and distinct day-to-day variation in isotope values of soil derived N<sub>2</sub>O,~~  
556 ~~especially in SP, were observed. Such changes were often strong and abrupt following~~  
557 ~~management events (Mant & III, Rewetting), indicating a significant response of microbial~~  
558 ~~processes to the imposed disturbance. Larger than expected variability in isotope values was~~  
559 ~~observed in-between management events (class BG), when no obvious variation in environmental~~  
560 ~~drivers occurred. Since noon-to-noon concentration increases were very small during these~~  
561 ~~periods, part of this variability may be attributed to increased uncertainty around the intercept of~~  
562 ~~the Keeling plot. This is also reflected in the relatively large error bars around isotope values on~~  
563 ~~days when overnight N<sub>2</sub>O concentration increase was low (Figure 3). Alternatively, the variation~~  
564 ~~in isotope values associated with small overnight concentration increase may result from other~~  
565 ~~land use or land cover. The EC fluxes are calculated from the turbulent fluctuation of~~

566 concentration and vertical wind speed (i.e. the covariance of the concentration and wind speed  
567 deviations from the half-hourly mean) and therefore account for the modulation of concentration  
568 around a short term (30 min) mean caused by locally emitted N<sub>2</sub>O. Isotopic composition based on  
569 Keeling plots however is determined from total N<sub>2</sub>O accumulated in the nocturnal boundary layer  
570 and, thus, this approach also contains molecules that had been emitted outside the flux footprint,  
571 which almost exclusively comprised our grassland site (Zeeman et al., 2010), within the larger  
572 concentration footprint (Griffis et al., 2007). However, two facts indicate a major influence of the  
573 studied grassland on the determined N<sub>2</sub>O isotopic composition: First, the N<sub>2</sub>O isotopic  
574 composition is very stable for a noon-to-noon period as indicated by a linear relationship between  
575 individual measurements (supplementary file S1). This relationship persists even though wind  
576 speed and direction are changing and, therefore, individual N<sub>2</sub>O isotope measurements integrating  
577 over 16 minutes sampling interval originate from different source areas. Secondly, the CHA  
578 grassland can be characterized as a site with vigorous N<sub>2</sub>O emission and therefore may dominate  
579 the determined N<sub>2</sub>O isotopic composition as the influence of a source area increment scales with  
580 the source strength. The grassland was restored in 2012 which lead to extraordinary high N<sub>2</sub>O-N  
581 emission of 29.1 kg ha<sup>-1</sup> year<sup>-1</sup> (Merbold et al., 2014). In the following year 2.5 kg N<sub>2</sub>O-N ha<sup>-1</sup>  
582 were released. This value is still in the range of maximum emissions reported for another  
583 intensively managed Swiss grassland, emitting 1.5-2.6 kg N ha<sup>-1</sup> year<sup>-1</sup> and at least a factor of five  
584 compared to an extensively managed grassland with less than 0.5 kg N ha<sup>-1</sup> year<sup>-1</sup> (Ammann et  
585 al., 2009). With regard to distant land use and land cover, the 2.5 kg N<sub>2</sub>O-N are also more than  
586 double the median (between the 70 and 75 percentile) of all reported values for cultivated  
587 temperate sites and higher than the highest value reported for forests presented in a study  
588 containing 1008 N<sub>2</sub>O emission measurements from agricultural fields (Stehfest and Bouwman,

589 2006). However, it cannot be excluded that N<sub>2</sub>O isotopic signatures analyzed above the grassland  
590 were influenced by adjacent ecosystems.

#### 591 4.7 Flux weighted averages of source isotopic compositions

592 N<sub>2</sub>O isotopic composition can be used to calculate and further constrain the global N<sub>2</sub>O budget  
593 (Kim and Craig, 1993; Yoshida and Toyoda, 2000). The analysis of emissions from different  
594 sources such as agricultural soils or managed grasslands based on box models and isotopic  
595 composition is complicated by distinct temporal and spatial variability of isotopic composition  
596 (Kim and Craig, 1993; Toyoda et al., 2011; Yoshida and Toyoda, 2000); hence, flux weighted  
597 averages are required to obtain representative values for agricultural N<sub>2</sub>O (Perez et al., 2001). Our  
598 flux weighted averages of  $6.9 \pm 4.3$ ,  $-17.4 \pm 6.2$  and  $27.4 \pm 3.6$  ‰ for SP,  $\delta^{15}\text{N}^{\text{bulk}}$  and  $\delta^{18}\text{O}$  are  
599 well within the range of values 2.9 to 36.6, -41.5 to -1.9 and 23.2 to 51.7 ‰ for agricultural soils  
600 (Park et al., 2011; Toyoda et al., 2011). The comparison with other grassland soils (Opdyke et al.,  
601 2009; Park et al., 2011) indicates that the variability of isotopic composition within a group, such  
602 as grassland, may be considerable (for SP: 2.2 to 11.1 ‰). Part One has to keep in mind, however,  
603 that part of the observed variability may be attributed to the fact that the footprint area of the N<sub>2</sub>O  
604 isotopic composition includes areas with other land use or land cover. Another part of the  
605 variability might be also explained by a limited compatibility of laboratory results, as recently  
606 demonstrated in an inter-laboratory comparison campaign (Mohn et al., 2014). The uncertainty in  
607 budgets derived by isotopic composition depends on the uncertainty of the representative isotopic  
608 composition for a single source, which can be reduced by a quasi-continuous measurement  
609 approach, as shown in this study.

## 610 5 Conclusion

611 Our field observations indicate that nitrifier-denitrification and denitrification (process group  
612  $N_2O_D$ ) dominated throughout the measurement period and that variation in isotopic composition  
613 was more likely due to variation in the extent of  $N_2O$  reduction rather than contributions of  
614  $NH_2OH$  oxidation- or fungal denitrification. High temporal resolution of isotopic composition in  
615 soil-emitted  $N_2O$  showed that at the beginning of the growing season, medium wfps and low  
616 temperature induced low isotope values (representative for process group  $N_2O_D$ ), whereas in the  
617 second part of the measurement period, higher temperature and DOC stimulated  $N_2O$  reduction to  
618  $N_2$ , although wfps was lower. Management or rewetting events were mostly characterized by low  
619 SP,  $\delta^{15}N^{bulk}$  and  $\delta^{18}O$ , but the event Mana II indicated that processes underlying  $N_2O$  emissions  
620 can vary even under similar management conditions. With this study, a new method is available  
621 that can provide real-time datasets for various single  $N_2O$  emitting (eco)systems, such as as  
622 grasslands or agriculturally used regions, which will help in further constraining the global  $N_2O$   
623 budget based on box model calculations. However, future campaigns should be accompanied by  
624 footprint modeling for optimization of the inlet height and associated concentration footprint size.  
625

626 **Acknowledgements**

627 We are grateful to Hans-Ruedi Wettstein and his team for the collaboration with the ETH  
628 research station Chamau and Christoph Zellweger for support with determination of GHG mixing  
629 ratios in our target gases. Antoine Roth is acknowledged for his support during the field  
630 campaign. This project was funded by the State Secretariat for Education and Research (SER)  
631 within COST Action ES0806. The QCLAS used for EC measurements was funded by the R'Equip  
632 Project (206021 133763) by the Swiss National Science Foundation. Funding from GHG-Europe  
633 (FP7, EU contract No. 244122) and COST Action ES0804 - ABBA is gratefully acknowledged.  
634 Instrumental developments at Empa were supported by the Swiss National Science Foundation  
635 (SNSF). Technical support on the eddy covariance station has been provided by Thomas Baur  
636 and Peter Plüss. Preparation of N<sub>2</sub>O isotope standards and inter-laboratory comparison  
637 measurements were supported by the EMRP ENV52 project 'Metrology for high-impact  
638 greenhouse gases'. The EMRP is jointly funded by the EMRP participating countries within  
639 EURAMET and the European Union.

640

641

642

643 **References**

644 Ammann, C., Spirig, C., Leifeld, J. and Neftel, A.: Assessment of the nitrogen and carbon budget  
645 of two managed temperate grassland fields, *Agric. Ecosyst. Environ.*, 133(3-4), 150–162,  
646 doi:10.1016/j.agee.2009.05.006, 2009.

647 Baggs, E. M.: A review of stable isotope techniques for N<sub>2</sub>O source partitioning in soils : recent  
648 progress , remaining challenges and future considerations, *Rapid Commun. Mass Spectrom.*, 22,  
649 1664–1672, doi:10.1002/rcm, 2008.

650 Baldocchi, D. and Meyers, T.: On using eco-physiological, micrometeorological and  
651 biogeochemical theory to evaluate carbon dioxide, water vapor and trace gas fluxes over  
652 vegetation: a perspective, *Agric. For. Meteorol.*, 90(1-2), 1–25, doi:10.1016/S0168-  
653 1923(97)00072-5, 1998.

654 Bedard-Haughn, A., van Groenigen, J. W. and van Kessel, C.: Tracing <sup>15</sup>N through landscapes:  
655 potential uses and precautions, *J. Hydrol.*, 272(1-4), 175–190, doi:10.1016/S0022-  
656 1694(02)00263-9, 2003.

657 Butterbach-Bahl, K., Baggs, E. M., Dannenmann, M., Kiese, R. and Zechmeister-Boltenstern, S.:  
658 Nitrous oxide emissions from soils : how well do we understand the processes and their controls?,  
659 *Philos. Trans. R. Soc. B-Biological Sci.*, 368, 20130122, 2013.

660 Davidson, E. A.: The contribution of manure and fertilizer nitrogen to atmospheric nitrous oxide  
661 since 1860, *Nat. Geosci.*, 2(9), 659–662, 2009.

662 Decock, C. and Six, J.: An assessment of N-cycling and sources of N<sub>2</sub>O during a simulated rain  
663 event using natural abundance <sup>15</sup>N, *Agric. , Ecosyst. Environ.*, 165, 141–150, 2013a.

664 Decock, C. and Six, J.: How reliable is the intramolecular distribution of <sup>15</sup>N in N<sub>2</sub>O to source  
665 partition N<sub>2</sub>O emitted from soil?, *Soil Biol. Biochem.*, 65(2), 114–127,  
666 doi:10.1016/j.soilbio.2013.05.012, 2013b.

667 Eugster, W. and Plüss, P.: A fault-tolerant eddy covariance system for measuring CH<sub>4</sub> fluxes,  
668 *Agric. For. Meteorol.*, 150(6), 841–851, doi:10.1016/j.agrformet.2009.12.008, 2010.

669 Griffis, T. J., Zhang, J., Baker, J. M., Kljun, N. and Billmark, K.: Determining carbon isotope  
670 signatures from micrometeorological measurements: Implications for studying biosphere–  
671 atmosphere exchange processes, *Boundary-Layer Meteorol.*, 123(2), 295–316,  
672 doi:10.1007/s10546-006-9143-8, 2007.

- 673 Groffman, P. M., Altabet, M. A., Bohlke, J. K., Butterbach-Bahl, K., David, M. B., Firestone, M.  
674 K., Giblin, A. E., Kana, T. M., Nielsen, L. P. and Voytek, M. A.: Methods for measuring  
675 denitrification: Diverse approaches to a difficult problem, *Ecol. Appl.*, 16(6), 2091–2122, 2006.
- 676 Harris, E., Nelson, D. D., Olszewski, W., Zahniser, M., Potter, K. E., McManus, B. J., Whitehill,  
677 A., Prinn, R. G. and Ono, S.: Development of a Spectroscopic Technique for Continuous Online  
678 Monitoring of Oxygen and Site-Specific Nitrogen Isotopic Composition of Atmospheric Nitrous  
679 Oxide., *Anal. Chem.*, doi:10.1021/ac403606u, 2014a.
- 680 Harris, E., Zeyer, K., Kegel, R., Müller, B., Emmenegger, L. and Mohn, J.: Nitrous oxide  
681 emissions and isotopic composition from waste incineration in Switzerland, *Waste Manag.*, in  
682 press, 2014b.
- 683 Heil, J., Wolf, B., Brüggemann, N., Emmenegger, L., Tuzson, B., Vereecken, H. and Mohn, J.:  
684 Site-specific <sup>15</sup>N isotopic signatures of abiotically produced N<sub>2</sub>O, *Geochim. Cosmochim. Acta*,  
685 139, 72–82, doi:10.1016/j.gca.2014.04.037, 2014.
- 686 Jinuntuya-Nortman, M., Sutka, R. L., Ostrom, P. H., Gandhi, H. and Ostrom, N. E.: Isotopologue  
687 fractionation during microbial reduction of N<sub>2</sub>O within soil mesocosms as a function of water-  
688 filled pore space, *Soil Biol. Biochem.*, 40(9), 2273–2280, doi:10.1016/j.soilbio.2008.05.016,  
689 2008.
- 690 Keeling, C. D.: The concentration and isotopic abundances of atmospheric carbon dioxide in  
691 rural areas, *Geochim. Cosmochim. Acta*, 13, 322–334, doi:10.1016/0016-7037(58)90033-4,  
692 1958.
- 693 Kim, K. R. and Craig, H.: Nitrogen-15 and oxygen-18 characteristics of nitrous oxide: a global  
694 perspective., *Science*, 262(5141), 1855–7, doi:10.1126/science.262.5141.1855, 1993.
- 695 Koba, K., Osaka, K., Tobari, Y., Toyoda, S., Ohte, N., Katsuyama, M., Suzuki, N., Itoh, M.,  
696 Yamagishi, H., Kawasaki, M., Kim, S. J., Yoshida, N. and Nakajima, T.: Biogeochemistry of  
697 nitrous oxide in groundwater in a forested ecosystem elucidated by nitrous oxide isotopomer  
698 measurements, *Geochim. Cosmochim. Acta*, 73(11), 3115–3133, doi:10.1016/j.gca.2009.03.022,  
699 2009.
- 700 Koehler, B., Corre, M. D., Steger, K., Well, R., Zehe, E., Sueta, J. P. and Veldkamp, E.: An in-  
701 depth look into a tropical lowland forest soil: nitrogen-addition effects on the contents of N<sub>2</sub>O,  
702 CO<sub>2</sub> and CH<sub>4</sub> and N<sub>2</sub>O isotopic signatures down to 2-m depth, *Biogeochemistry*, 111(1-3), 695–  
703 713, doi:10.1007/s10533-012-9711-6, 2012.
- 704 Kool, D. M., Wrage, N., Oenema, O., Harris, D. and Groenigen, J. W. Van: The <sup>18</sup>O signature of  
705 biogenic nitrous oxide is determined by O exchange with water, *Rapid Commun. Mass*  
706 *Spectrom.*, 23, 104–108, doi:10.1002/rcm, 2009.
- 707 Köster, J. R., Cárdenas, L., Senbayram, M., Bol, R., Well, R., Butler, M., Mühling, K. H. and  
708 Dittert, K.: Rapid shift from denitrification to nitrification in soil after biogas residue application

709 as indicated by nitrous oxide isotopomers, *Soil Biol. Biochem.*, 43(8), 1671–1677,  
710 doi:10.1016/j.soilbio.2011.04.004, 2011.

711 Köster, J. R., Well, R., Dittert, K., Giesemann, A., Lewicka-Szczebak, D., Mühling, K.-H.,  
712 Herrmann, A., Lammel, J. and Senbayram, M.: Soil denitrification potential and its influence on  
713 N<sub>2</sub>O reduction and N<sub>2</sub>O isotopomer ratios., *Rapid Commun. mass Spectrom.*, 27(21), 2363–73,  
714 doi:10.1002/rcm.6699, 2013a.

715 Köster, J. R., Well, R., Tuzson, B., Bol, R., Dittert, K., Giesemann, A., Emmenegger, L.,  
716 Manninen, A., Cárdenas, L. and Mohn, J.: Novel laser spectroscopic technique for continuous  
717 analysis of N<sub>2</sub>O isotopomers--application and intercomparison with isotope ratio mass  
718 spectrometry., *Rapid Commun. Mass Spectrom.*, 27(1), 216–22, doi:10.1002/rcm.6434, 2013b.

719 Lewicka-Szczebak, D., Well, R., Bol, R., Gregory, A. S., Matthews, G. P., Misselbrook, T.,  
720 Whalley, W. R. and Cardenas, L. M.: Isotope fractionation factors controlling isotopocule  
721 signatures of soil-emitted N<sub>2</sub>O produced by denitrification processes of various rates, *Rapid*  
722 *Commun. Mass Spectrom.*, 29, 269–282, doi:10.1002/rcm.7102, 2015.

723 Lewicka-Szczebak, D., Well, R., Köster, J. R., Fuß, R., Senbayram, M., Dittert, K. and Flessa,  
724 H.: Experimental determinations of isotopic fractionation factors associated with N<sub>2</sub>O production  
725 and reduction during denitrification in soils, *Geochim. Cosmochim. Acta*, 134, 55–73,  
726 doi:10.1016/j.gca.2014.03.010, 2014.

727 Merbold, L., Eugster, W., Stieger, J., Zahniser, M., Nelson, D. and Buchmann, N.: Greenhouse  
728 gas budget (CO<sub>2</sub>, CH<sub>4</sub> and N<sub>2</sub>O) of intensively managed grassland following restoration., *Glob.*  
729 *Chang. Biol.*, 20(6), 1913–1928, doi:10.1111/gcb.12518, 2014.

730 Mohn, J., Guggenheim, C., Tuzson, B., Vollmer, M. K., Toyoda, S., Yoshida, N. and  
731 Emmenegger, L.: A liquid nitrogen-free preconcentration unit for measurements of ambient N<sub>2</sub>O  
732 isotopomers by QCLAS, *Atmos. Meas. Tech.*, 3(3), 609–618, doi:10.5194/amt-3-609-2010,  
733 2010.

734 Mohn, J., Steinlin, C., Merbold, L., Emmenegger, L. and Hagedorn, F.: N<sub>2</sub>O emissions and  
735 source processes in snow-covered soils in the Swiss Alps., *Isotopes Environ. Health Stud.*, 49(4),  
736 520–31, doi:10.1080/10256016.2013.826212, 2013.

737 Mohn, J., Tuzson, B., Manninen, A., Yoshida, N., Toyoda, S., Brand, W. A. and Emmenegger,  
738 L.: Site selective real-time measurements of atmospheric N<sub>2</sub>O isotopomers by laser spectroscopy,  
739 *Atmos. Meas. Tech.*, 5(7), 1601–1609, doi:10.5194/amt-5-1601-2012, 2012.

740 Mohn, J., Wolf, B., Toyoda, S., Lin, C. T., Liang, C. M., Brüggemann, N., Wissel, H., Steiker, A.  
741 E., Dyckmans, J., Szwek, L., Ostrom, N. E., Casciotti, K. L., Forbes, M., Giesemann, A., Well,  
742 R., Doucett, R. R., Yarnes, C. T., Ridley, A. R., Kaiser, J. and Yoshida, N.: Inter-Laboratory  
743 assessment of notrous oxide isotopomer analysis of isotopomer analysis by isotope ratio mass  
744 spectrometry and laser spectroscopy: current status and perspectives, *Rapid Commun. Mass*  
745 *Spectrom.*, 28, 1995–2007, 2014.



746 Mosier, A., Kroeze, C., Nevison, C., Oenema, O., Seitzinger, S. and van Cleemput, O.: Closing  
747 the global N<sub>2</sub>O budget: nitrous oxide emissions through the agricultural nitrogen cycle -  
748 OECD/IPCC/IEA phase II development of IPCC guidelines for national greenhouse gas  
749 inventory methodology, *Nutr. Cycl. Agroecosystems*, 52(2-3), 225–248, 1998.

750 Myhre, G., Shindell, D., Bréon, F.-M., Collins, W., Fuglestedt, J., Huang, J., Koch, D.,  
751 Lamarque, L., Mendoza, B., Nakaijima, T., Robock, A., Stephens, G., Takemura, T. and Zhang,  
752 H.: Anthropogenic and Natural Radiative Forcing, in *Climate Change 2013: The Physical  
753 Science Basis. Contribution of Working Group I to the Fifth Assessment Report of the  
754 Intergovernmental Panel on Climate Change*, edited by T. Stocker, D. Qin, P. GK, M. Tignor, S.  
755 Allen, J. Boschung, A. Nauels, Y. Xia, V. Bex, and P. Midgley, pp. 659–740, Cambridge  
756 University Press, Cambridge, UK and New York, NY, USA., 2013.

757 Ogawa, M. and Yoshida, N.: Intramolecular distribution of stable nitrogen and oxygen isotopes  
758 of nitrous oxide emitted during coal combustion., *Chemosphere*, 61(6), 877–87,  
759 doi:10.1016/j.chemosphere.2005.04.096, 2005.

760 Opdyke, M. R., Ostrom, N. E. and Ostrom, P. H.: Evidence for the predominance of  
761 denitrification as a source of N<sub>2</sub>O in temperate agricultural soils based on isotopologue  
762 measurements, *Global Biogeochem. Cycles*, 23(4), GB4018 1–10, doi:10.1029/2009GB003523,  
763 2009.

764 Ostrom, N. E. and Ostrom, P. H.: The Isotopomers of Nitrous Oxide: Analytical Considerations  
765 and Application to Resolution of Microbial Production Pathways, in *Handbook of  
766 Environmental Isotope Geochemistry Volume 1*, edited by M. Baskaran, pp. 453–476, Springer  
767 Berlin Heidelberg, Berlin, Heidelberg., 2011.

768 Ostrom, N. E., Pitt, A., Sutka, R. L., Ostrom, P. H., Grandy, A. S., Huizinga, K. M. and  
769 Robertson, G. P.: Isotopologue effects during N<sub>2</sub>O reduction in soils and in pure cultures of  
770 denitrifiers, *J. Geophys. Res.*, 112(G2), 1–12, doi:10.1029/2006JG000287, 2007.

771 Ostrom, N. E., Sutka, R. L., Ostrom, P. H., Grandy, A. S., Huizinga, K. M., Gandhi, H., von  
772 Fischer, J. C. and Robertson, G. P.: Isotopologue data reveal bacterial denitrification as the  
773 primary source of N<sub>2</sub>O during a high flux event following cultivation of a native temperate  
774 grassland, *Soil Biol. Biochem.*, 42(3), 499–506, doi:10.1016/j.soilbio.2009.12.003, 2010.

775 Park, S., Pérez, T., Boering, K. A., Trumbore, S. E., Gil, J., Marquina, S. and Tyler, S. C.: Can  
776 N<sub>2</sub>O stable isotopes and isotopomers be useful tools to characterize sources and microbial  
777 pathways of N<sub>2</sub>O production and consumption in tropical soils?, *Global Biogeochem. Cycles*,  
778 25(1), 1–16, doi:10.1029/2009GB003615, 2011.

779 Pataki, D., Ehleringer, J., Flanagan, L., Yakir, D., Bowling, D., Still, C., Buchmann, N., Kaplan,  
780 J. and Berry, J.: The application and interpretation of Keeling plots in terrestrial carbon cycle  
781 research, *Global Biogeochem. Cycles*, 17(1), doi:10.1029/2001GB001850, 2003.

- 782 Perez, T., Garcia-Montiel, D. C., Trumbore, S. E., Tyler, S., de Camargo, P. B., Moreira, M.,  
783 Piccolo, M. C. and Cerri, C.: Nitrous Oxide Nitrification and Denitrification <sup>15</sup>N Enrichment  
784 Factors from Amazon Forest Soils, *Ecol. Appl.*, 16(6), 2153–2167, 2006.
- 785 Perez, T., Trumbore, S. E., Tyler, S. C., Matson, P. A., Ortiz-Monasterio, I., Rahn, T. and  
786 Griffith, D. W. T.: Identifying the agricultural imprint on the global N<sub>2</sub>O budget using stable  
787 isotopes, *J. Geophys. Res.*, 106(D9), 9869–9878, 2001.
- 788 Ravishankara, A. R., Daniel, J. S. and Portmann, R. W.: Nitrous oxide (N<sub>2</sub>O): the dominant  
789 ozone-depleting substance emitted in the 21st century., *Science* (80)., 326(5949), 123–5,  
790 doi:10.1126/science.1176985, 2009.
- 791 Roth, K.: *Bodenkartierung und GIS-basierte Kohlenstoffinventur von Graslandböden*, 132 pp.,  
792 University of Zürich (UZH)., 2006.
- 793 Sagar, S., Jha, N., Deslippe, J., Bolan, N. S., Luo, J., Giltrap, D. L., Kim, D.-G., Zaman, M. and  
794 Tillman, R. W.: Denitrification and N<sub>2</sub>O:N<sub>2</sub> production in temperate grasslands: processes,  
795 measurements, modelling and mitigating negative impacts., *Sci. Total Environ.*, 465, 173–95,  
796 doi:10.1016/j.scitotenv.2012.11.050, 2013.
- 797 Stehfest, E. and Bouwman, L.: N<sub>2</sub>O and NO emission from agricultural fields and soils under  
798 natural vegetation: summarizing available measurement data and modeling of global annual  
799 emissions, *Nutr. Cycl. Agroecosystems*, 74(3), 207–228, 2006.
- 800 Sutka, R. L., Adams, G. C., Ostrom, N. E. and Ostrom, P. H.: Isotopologue fractionation during  
801 N<sub>2</sub>O production by fungal denitrification, *Rapid Commun. Mass Spectrom.*, 22, 3989–3996,  
802 doi:10.1002/rcm, 2008.
- 803 Sutka, R. L., Ostrom, N. E., Ostrom, P. H., Breznak, J. A., Pitt, A. J., Li, F. and Gandhi, H.:  
804 Distinguishing Nitrous Oxide Production from Nitrification and Denitrification on the Basis of  
805 Isotopomer Abundances, *Appl. Environ. Microbiol.*, 72(1), 638–644, doi:10.1128/AEM.72.1.638,  
806 2006.
- 807 Sutka, R. L., Ostrom, N. E., Ostrom, P. H., Gandhi, H. and Breznak, J. a: Nitrogen isotopomer  
808 site preference of N<sub>2</sub>O produced by *Nitrosomonas europaea* and *Methylococcus capsulatus* Bath.,  
809 *Rapid Commun. Mass Spectrom.*, 17(7), 738–45, doi:10.1002/rcm.968, 2003.
- 810 Syakila, A. and Kroeze, C.: The global nitrous oxide budget revisited, *Greenh. Gas Meas.*  
811 *Manag.*, 1(1), 17–26, doi:10.3763/ghgmm.2010.0007, 2011.
- 812 Toyoda, S., Kuroki, N., Yoshida, N., Ishijima, K., Tohjima, Y. and Machida, T.: Decadal time  
813 series of tropospheric abundance of N<sub>2</sub>O isotopomers and isotopologues in the Northern  
814 Hemisphere obtained by the long-term observation at Hateruma Island, Japan, *J. Geophys. Res.*  
815 *Atmos.*, 118(8), 3369–3381, doi:10.1002/jgrd.50221, 2013.

- 816 Toyoda, S., Mutoke, H., Yamagishi, H., Yoshida, N. and Tanji, Y.: Fractionation of N<sub>2</sub>O  
817 isotopomers during production by denitrifier, *Soil Biol. Biochem.*, 37(8), 1535–1545,  
818 doi:10.1016/j.soilbio.2005.01.009, 2005.
- 819 Toyoda, S., Yano, M., Nishimura, S., Akiyama, H., Hayakawa, A., Koba, K., Sudo, S., Yagi, K.,  
820 Makabe, A., Tobar, Y., Ogawa, N. O., Ohkouchi, N., Yamada, K. and Yoshida, N.:  
821 Characterization and production and consumption processes of N<sub>2</sub>O emitted from temperate  
822 agricultural soils determined via isotopomer ratio analysis, *Global Biogeochem. Cycles*, 25(2), 1–  
823 17, doi:10.1029/2009GB003769, 2011.
- 824 Toyoda, S. and Yoshida, N.: Determination of Nitrogen Isotopomers of Nitrous Oxide on a  
825 Modified Isotope Ratio Mass Spectrometer, *Anal. Chem.*, 71(20), 4711–4718, 1999.
- 826 Tuzson, B., Zeyer, K., Steinbacher, M., McManus, J. B., Nelson, D. D., Zahniser, M. S. and  
827 Emmenegger, L.: Selective measurements of NO, NO<sub>2</sub> and NO<sub>y</sub> in the free troposphere using  
828 quantum cascade laser spectroscopy, *Atmos. Meas. Tech.*, 6(4), 927–936, doi:10.5194/amt-6-  
829 927-2013, 2013.
- 830 Waechter, H., Mohn, J., Tuzson, B., Emmenegger, L. and Sigrist, M. W.: Determination of N<sub>2</sub>O  
831 isotopomers with quantum cascade laser based absorption spectroscopy., *Opt. Express*, 16(12),  
832 9239–44, 2008.
- 833 Watts, S. H. and Seitzinger, S. P.: Denitrification rates in organic and mineral soils from riparian  
834 sites : a comparison of N<sub>2</sub> flux and acetylene inhibition methods, *Soil Biol. Biochem.*, 32, 1383–  
835 1392, 2000.
- 836 Well, R., Eschenbach, W., Flessa, H., von der Heide, C. and Weymann, D.: Are dual isotope and  
837 isotopomer ratios of N<sub>2</sub>O useful indicators for N<sub>2</sub>O turnover during denitrification in nitrate-  
838 contaminated aquifers?, *Geochim. Cosmochim. Acta*, 90, 265–282,  
839 doi:10.1016/j.gca.2012.04.045, 2012.
- 840 Well, R. and Flessa, H.: Isotopologue enrichment factors of N<sub>2</sub>O reduction in soils, *Rapid*  
841 *Commun. Mass Spectrom.*, 23, 2996–3002, doi:10.1002/rcm, 2009a.
- 842 Well, R. and Flessa, H.: Isotopologue signatures of N<sub>2</sub>O produced by denitrification in soils, *J.*  
843 *Geophys. Res.*, 114(G2), 1–11, doi:10.1029/2008JG000804, 2009b.
- 844 Well, R., Flessa, H., Xing, L., Xiaotang, J. and Römheld, V.: Isotopologue ratios of N<sub>2</sub>O emitted  
845 from microcosms with NH<sub>4</sub><sup>+</sup> fertilized arable soils under conditions favoring nitrification, *Soil*  
846 *Biol. Biochem.*, 40(9), 2416–2426, doi:10.1016/j.soilbio.2008.06.003, 2008.
- 847 Well, R., Kurganova, I., Lopesdegerenyu, V. and Flessa, H.: Isotopomer signatures of soil-  
848 emitted N<sub>2</sub>O under different moisture conditions—A microcosm study with arable loess soil, *Soil*  
849 *Biol. Biochem.*, 38(9), 2923–2933, doi:10.1016/j.soilbio.2006.05.003, 2006.
- 850 Wrage, N., Velthof, G. L., van Beusichem, M. L. and Oenema, O.: Role of nitrifier denitrification  
851 in the production of nitrous oxide, *Soil Biol. Biochem.*, 33(12-13), 1723–1732, 2001.

- 852 Wu, H., Dannenmann, M. D., Wolf, B., Han, X. G., Zheng, X. and Butterbach-Bahl, K.:  
853 Seasonality of soil microbial nitrogen turnover in continental steppe soils of Inner Mongolia,  
854 *Ecosphere*, 3(4), 34, 2012.
- 855 Wunderlin, P., Lehmann, M. F., Siegrist, H., Tuzson, B., Joss, A., Emmenegger, L. and Mohn, J.:  
856 Isotope signatures of N<sub>2</sub>O in a mixed microbial population system: constraints on N<sub>2</sub>O producing  
857 pathways in wastewater treatment., *Environ. Sci. Technol.*, 47(3), 1339–48,  
858 doi:10.1021/es303174x, 2013.
- 859 Wunderlin, P., Mohn, J., Joss, A., Emmenegger, L. and Siegrist, H.: Mechanisms of N<sub>2</sub>O  
860 production in biological wastewater treatment under nitrifying and denitrifying conditions.,  
861 *Water Res.*, 46(4), 1027–37, doi:10.1016/j.watres.2011.11.080, 2012.
- 862 Yamulki, S., Toyoda, S., Yoshida, N., Veldkamp, E., Grant, B. and Bol, R.: Diurnal fluxes and  
863 the isotopomer ratios of N<sub>2</sub>O in a temperate grassland following urine amendment., *Rapid*  
864 *Commun. Mass Spectrom.*, 15(15), 1263–9, doi:10.1002/rcm.352, 2001.
- 865 Yoshida, N. and Toyoda, S.: Constraining the atmospheric N<sub>2</sub>O budget from intramolecular site  
866 preference in N<sub>2</sub>O isotopomers, *Nature*, 405(6784), 330–4, doi:10.1038/35012558, 2000.
- 867 Zeeman, M., Hiller, R., Gilgen, A. K., Michna, P., Plüss, P., Buchmann, N. and Eugster, W.:  
868 Management and climate impacts on net CO<sub>2</sub> fluxes and carbon budgets of three grasslands along  
869 an elevational gradient in Switzerland, *Agric. For. Meteorol.*, 150(4), 519–530,  
870 doi:10.1016/j.agrformet.2010.01.011, 2010.

871

872

873

874 **Tables**

875 **Table 1: Reference gas and compressed air tanks used during the campaign. S1 and S2 represent the anchor and**  
876 **calibration standard. C1 and C2 are the target gases used for determination of system performance. The reported**  
877 **precision is the 1 $\sigma$  standard deviation.**

<b>Tank</b>	$\delta^{15}\text{N}^{\alpha}$ [‰]	$\delta^{15}\text{N}^{\beta}$ [‰]	$\delta^{18}\text{O}$ [‰]	$\delta^{15}\text{N}^{\text{bulk}}$ [‰]	<b>SP</b> [‰]	<b>mixing ratio</b> [ppm] / [ppb]*
<b>S1</b>	15.66 $\pm$ 0.03	-3.22 $\pm$ 0.13	34.89 $\pm$ 0.05	6.22 $\pm$ 0.07	18.88 $\pm$ 0.13	90.09 $\pm$ 0.01
<b>S2</b>	10.38 $\pm$ 0.03	-10.55 $\pm$ 0.1	25.44 $\pm$ 0.06	-0.09 $\pm$ 0.05	20.93 $\pm$ 0.10	87.28 $\pm$ 0.003
<b>C1</b>	15.40 $\pm$ 0.08	-3.04 $\pm$ 0.06	43.65 $\pm$ 0.08	6.18 $\pm$ 0.05	18.44 $\pm$ 0.10	327.01 $\pm$ 0.05
<b>C2</b>	15.65 $\pm$ 0.17	-4.27 $\pm$ 0.08	44.20 $\pm$ 0.07	5.69 $\pm$ 0.09	19.92 $\pm$ 0.19	327.45 $\pm$ 0.05

878 \* ppm for S1 and S2, ppb for C1, C2

879

880

881

882 **Table 2: Adjusted  $r^2$  and p-values for regression analysis of Keeling-plot derived isotopic compositions in soil-emitted  $N_2O$**   
 883 **versus auxiliary variables  $N_2O$  flux ( $f_{N_2O}$ ), difference of maximum and minimum concentration over a noon-to-noon**  
 884 **period ( $\Delta N_2O$ ), precipitation (prcp), soil moisture (wfps) and nutrient concentrations ( $NO_3^-$ ,  $NH_4^+$  and DOC).**  
 885

<b>explanatory</b>	<b>SP</b>	<b>SP</b>	<b><math>\delta^{15}N^{bulk}</math></b>	<b><math>\delta^{15}N^{bulk}</math></b>	<b><math>\delta^{18}O</math></b>	<b><math>\delta^{18}O</math></b>	<b>N</b>
	<b><math>r^2</math></b>	<b>p</b>	<b><math>r^2</math></b>	<b>p</b>	<b><math>r^2</math></b>	<b>p</b>	
<b><math>f_{N_2O}</math></b>	0.14	**	0.04	0.06	0.16	**	62
<b><math>\Delta N_2O</math></b>	0.09	*	0.1	*	0.11	*	65
<b>prcp</b>	0.24	**	0.03	0.08	0.24	**	62
<b>wfps</b>	0.14	*	0.29	**	-0.009	0.52	65
<b>T</b>	0.22	**	0.30	**	0.12	*	65
<b>DOC</b>	0.23	*	0.30	*	0.03	0,23	18
<b><math>NO_3^-</math></b>	0.04	0.14	0.27	*	0.16	*	31
<b><math>NH_4^+</math></b>	-0.03	0.75	-0.03	0.89	-0.03	0.93	31
<b>Significance codes: *: <math>p &lt; 0.05</math>; **: <math>p &lt; 0.001</math>. sample size (n) differs due to data availabilities.</b>							

886

887

888 **Figure legends**

889 **Figure 1:** Long-term stability (standard deviation  $\sigma$ ) derived by target gas injections (n=331) over a 3-month period.

890 As two target gas tanks were used, histograms show deviation of respective tank means,  $\bar{x}$ , for  $\delta^{15}\text{N}^\alpha$ ,  $\delta^{15}\text{N}^\beta$ ,  $\delta^{18}\text{O}$ ,

891  $\delta^{15}\text{N}^{\text{bulk}}$  and SP, respectively

892

893 **Figure 2:** Target gas (red) and surface layer (black)  $\text{N}_2\text{O}$  mole fractions (top) and  $\delta$ -values (three bottom panels)

894 measured in the atmospheric surface layer in 2.2 m height during the field campaign. Each couple of vertical dashed

895 blue lines indicates the management events mowing (first line) and fertilization (second line).

896

897 **Figure 3:** Noon-to-noon averaged  $\text{N}_2\text{O}$  flux ( $f_{\text{N}_2\text{O}}$ ), overnight increase in  $\text{N}_2\text{O}$  mole fractions (difference in minimum

898 and maximum  $\text{N}_2\text{O}$  concentration in a noon-to-noon period;  $\delta\text{N}_2\text{O}$ ), Keeling-plot derived isotopic composition of

899 soil-emitted  $\text{N}_2\text{O}$  (SP,  $\delta^{15}\text{N}^{\text{bulk}}$ ,  $\delta^{18}\text{O}$ ), nutrient concentrations (ammonium, nitrate and dissolved organic carbon;

900 DOC), water filled pore space (wfps), precipitation (prcp) and soil temperature (T) over the measurement period.

901 Each couple of vertical dashed blue lines indicates the management events mowing (first line) and fertilization

902 (second line). Transparent blue boxes represent periods of  $\text{N}_2\text{O}$  emission influenced by management or rewetting

903 (third box).

904

905 **Figure 4:** Standard error for SP ( $\epsilon_{\text{SP}}$ ) of soil-derived  $\text{N}_2\text{O}$  estimated by the Keeling plot approach as function of

906 overnight  $\text{N}_2\text{O}$  accumulation in the surface layer. The red dashed lines show 12 ppb increase in  $\text{N}_2\text{O}$  mole fractions.

907 Red full circles represent the selected subset.

908

909 **Figure 5:** SP -  $\text{NH}_4^+$  /  $\text{NO}_3^-$  and SP - wfps / soil temperature maps. The size of the points is inversely scaled to

910 Keeling plot intercept standard error so that biggest points are those with lowest uncertainty.

911

912 **Figure 6:** Boxplots for Keeling-plot derived SP,  $\delta^{15}\text{N}^{\text{bulk}}$ ,  $\delta^{18}\text{O}$  of soil-emitted  $\text{N}_2\text{O}$  and wfps of management events  
913 (Mana I – III), rainfall after a dry period (Rewetting), and the remaining measurement period (BG).

914

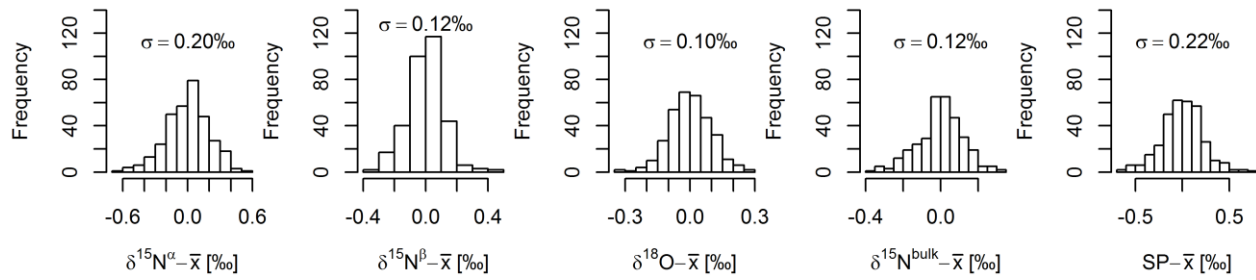
915 **Figure 7:** ~~Map~~ Left panel: map of  $\text{N}_2\text{O}$  isotopic composition  $\text{SP}/\delta^{15}\text{N}^{\text{bulk}}$  with rectangles representing process groups  
916  $\text{N}_2\text{O}_\text{N}$  and  $\text{N}_2\text{O}_\text{D}$  based on SP values in Decock and Six (2013, 2013b) and  $\delta^{15}\text{N}^{\text{bulk}}$  estimated from minimum and  
917 maximum fractionation factors reported in Baggs (2008) and substrate isotopic compositions reported by Bedard-  
918 Haughn et al (2003), Pörtl et al. (2007) and Toyoda et al. (2011). Right panel: map of  $\text{SP}/\delta^{18}\text{O}$  with traces of  
919 management events (ManaI in black, ManaII in red, ManaIII in green) and the rewetting event (blue). Isotopic  
920 compositions are plotted for the transparent blue boxes in Fig. 3 including one preceding and one following  
921 composition. The preceding composition is represented by the enlarged filled triangle and transparency of the line  
922 connecting the compositions decreases with event duration.

923

924

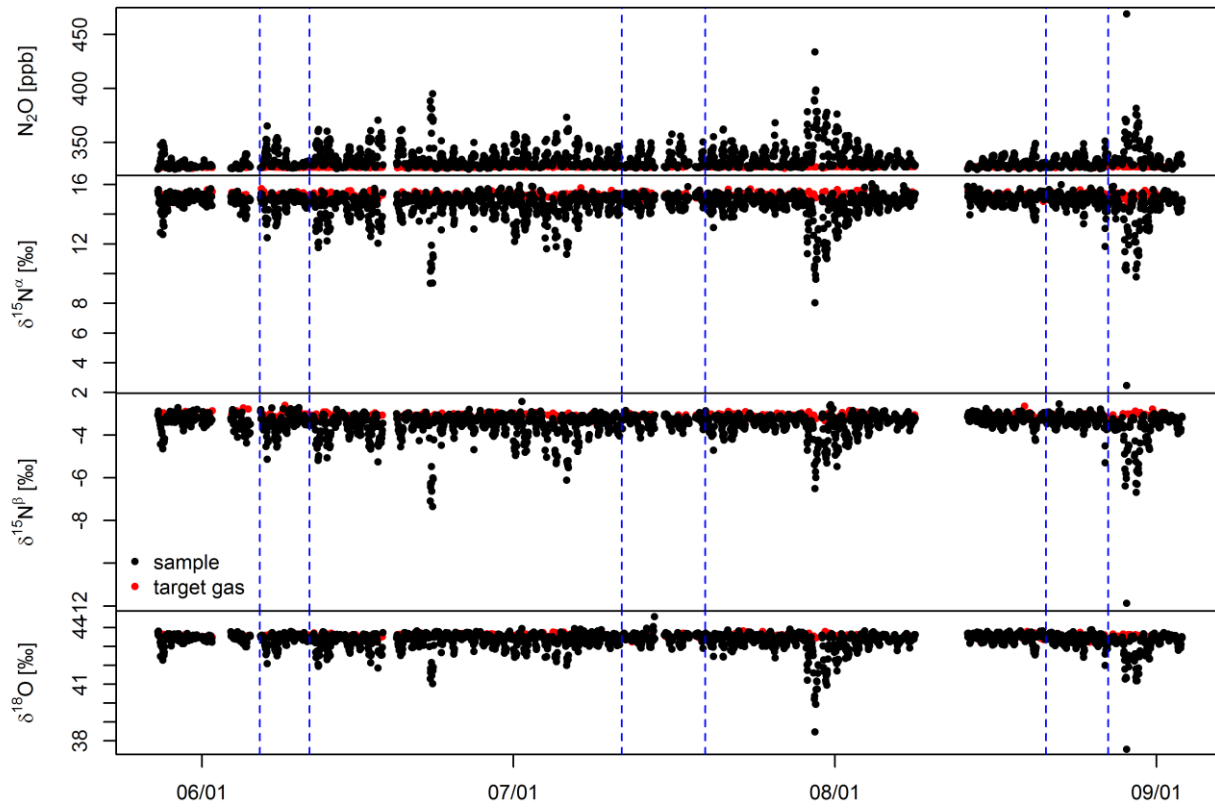


925 **Figures**



926

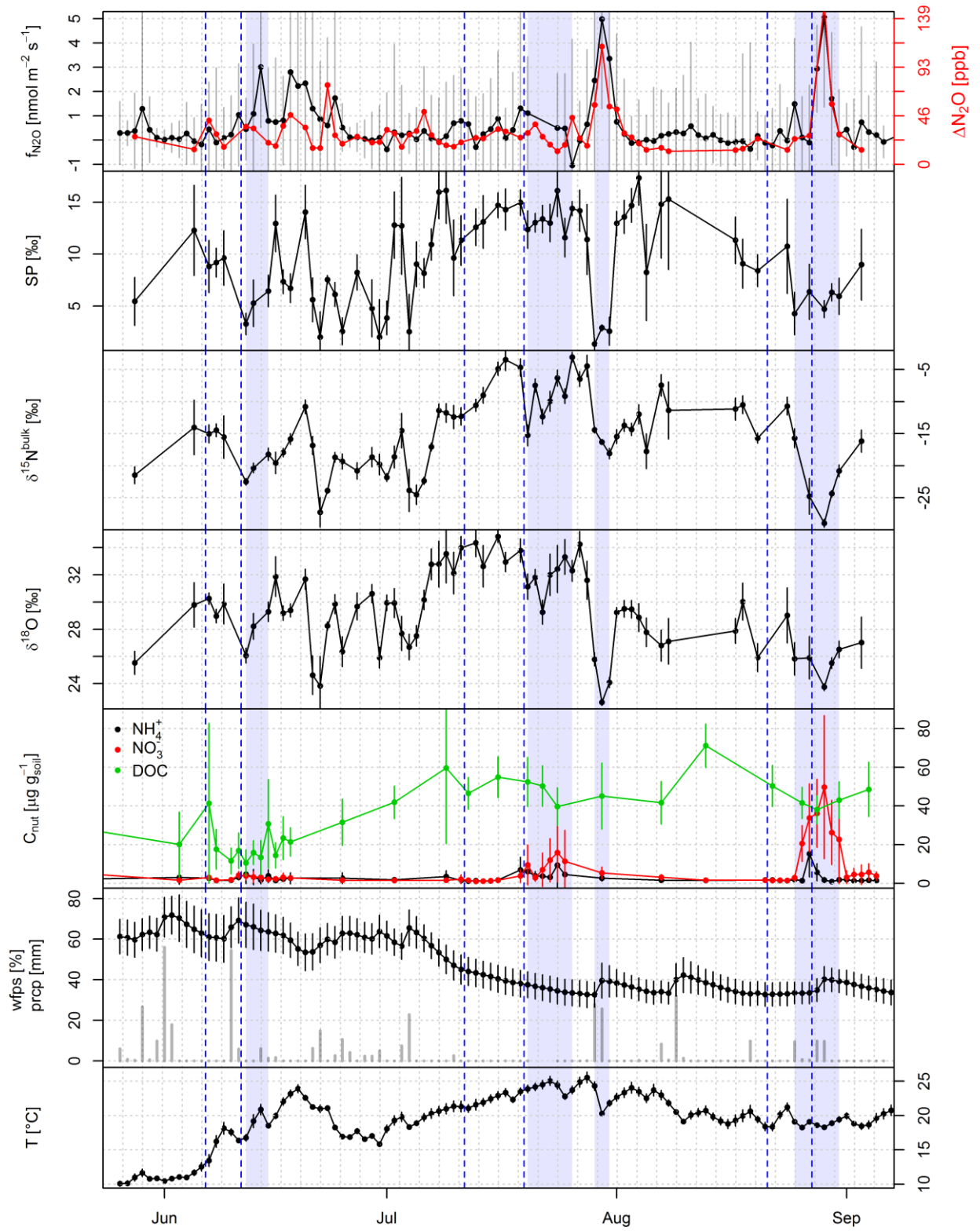
927 **Figure 1**



928

929 **Figure 2**

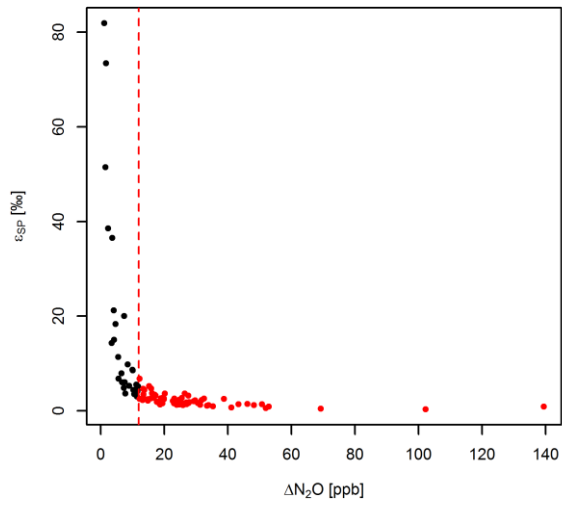
930



931

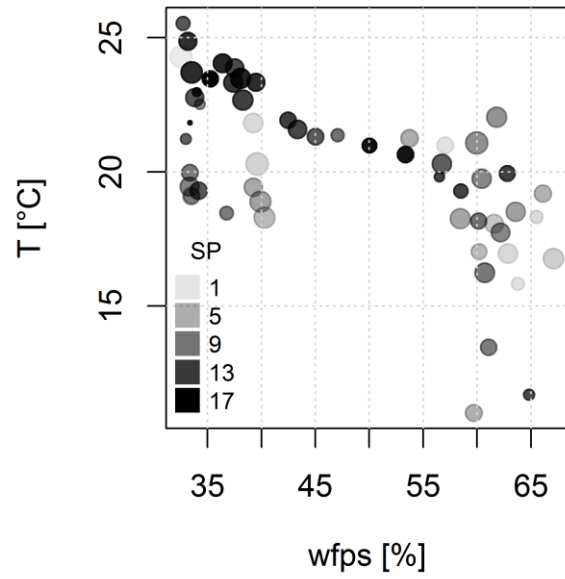
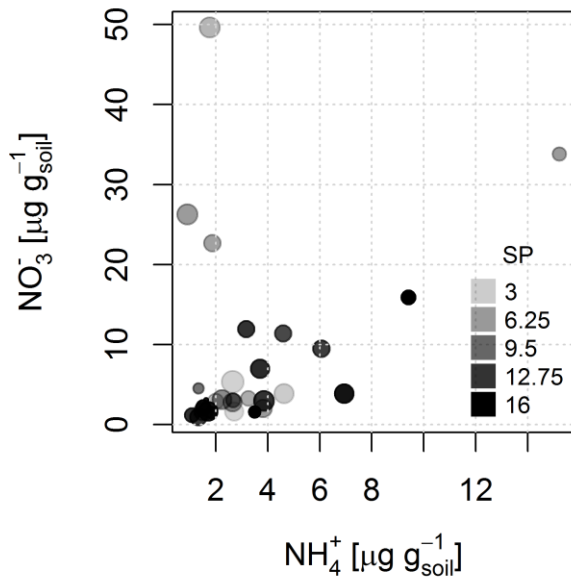
932 Figure 3

933



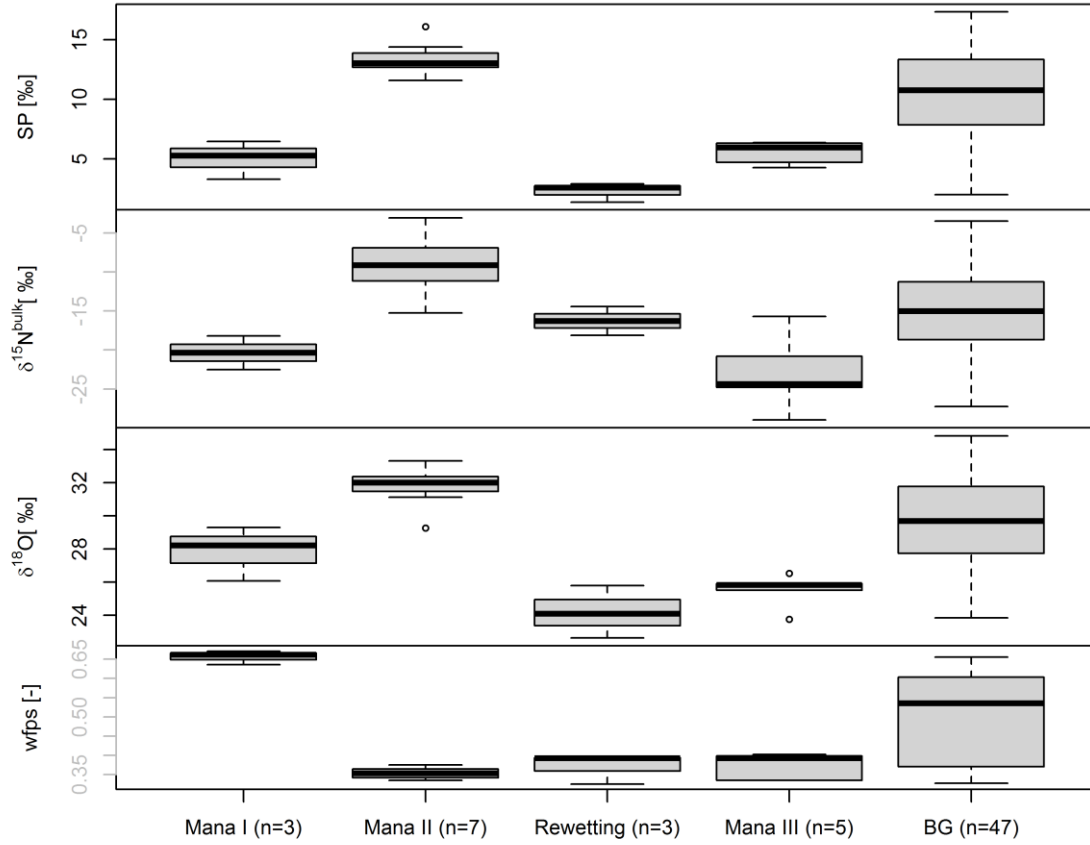
934

935 Figure 4



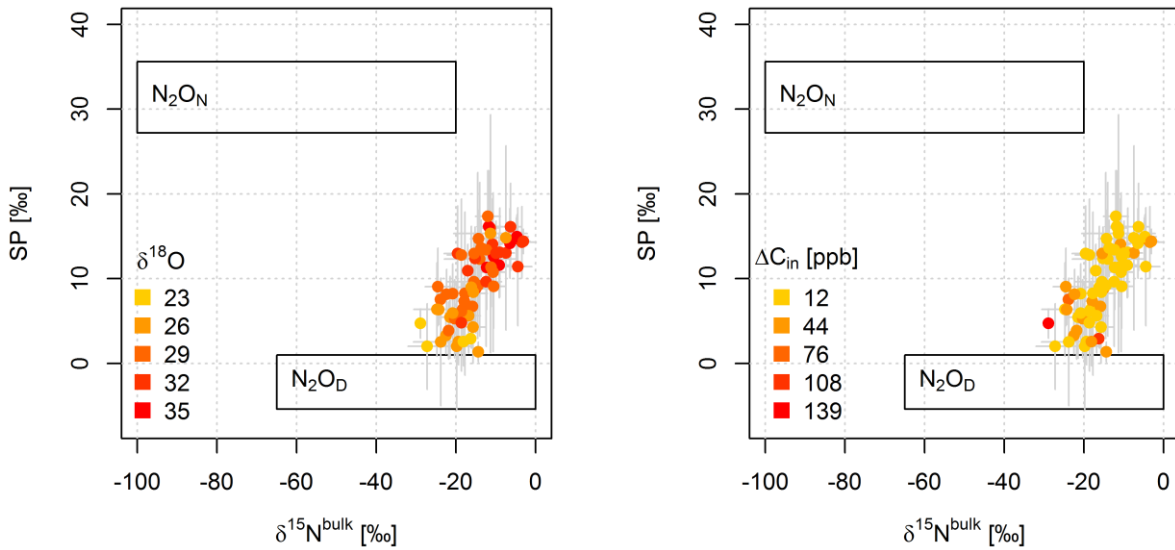
936

937 Figure 5



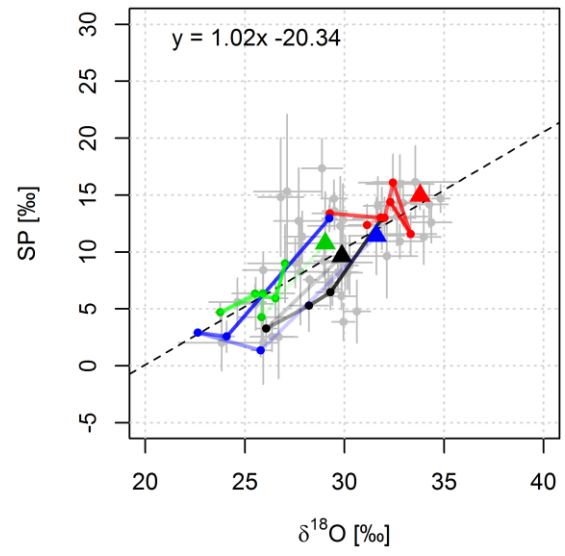
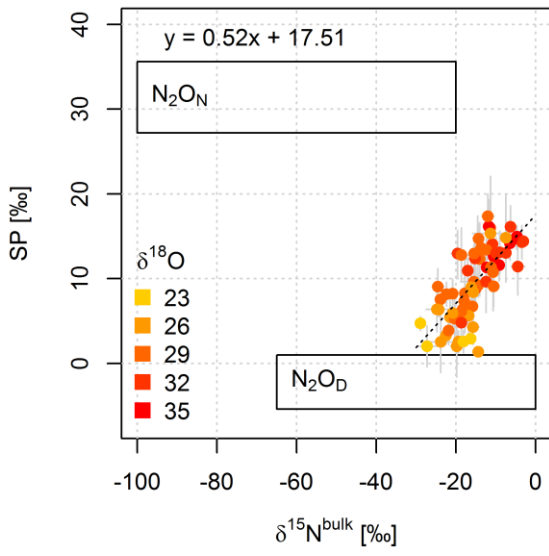
938

939 Figure 6



940

941



942

943 Figure 7